Low planktic foraminiferal diversity and abundance observed in a spring 2013 West-East Mediterranean Sea plankton tow transect

Miguel Mallo[1], Patrizia Ziveri[1,2], P. Graham Mortyn[1,3], Ralf Schiebel[4] and Michael Grelaud[1]

1. Institute of Environmental Science and Technology (ICTA), Autonomous University of Barcelona (UAB), Bellaterra 08193, Spain
2. Catalan Institution for Research and Advanced Studies (ICREA), Pg. Lluís Companys 23, 08010 Barcelona, Spain
3. Geography Department, UAB, Bellaterra 08193, Spain
4. LPG-BIAF, University of Angers, 2 bd Lavoisier, 49045 Angers, France, now at Climate Geochemistry, Max Planck Institute for Chemistry, Hahn-Meitner-Weg 1, 55128 Mainz, Germany

Abstract

Planktic foraminifera were collected with 150 μm BONGO nets from the upper 200 m water depth at 20 stations across the Mediterranean Sea between 02 May and 02 June, 2013. The main aim was to characterize the species distribution and the area density (ρ_A). Average foraminifera abundances are 1.42 ±1.43 ind.·10 m^{-3} (ranging from 0.11 to 5.20 ind.·10 m^{-3}), with a total of twelve morphospecies found. Large differences in species assemblages and absolute abundances are observed between the different Mediterranean sub-basins, with an overall dominance of spinose, symbiont-bearing species indicating oligotrophic conditions. The highest values in absolute abundance were found in the Strait of Gibraltar and the Alboran Sea. The western basin is dominated by *Globorotalia inflata* and *Globigerina bulloides* at slightly lower standing stocks than in the eastern basin. In contrast, the planktic foraminiferal assemblage in the warmer, saltier and more nutrient-limited eastern basin is dominated by *Globigerinoides ruber* (white). These new results in combination with comparison to previous findings, suggest that temperature-induced stratification of the surface water column, nutrient concentration and hence food availability, seem to be the main factors controlling foraminiferal abundances and distribution. In the highly alkaline and supersaturated with respect to calcite and aragonite Mediterranean surface water, standing stocks and ρ_A of *G. ruber* (white) and *G. bulloides* are affected by food availability and only secondarily by seawater carbonate chemistry. Increasing temperature, salinity, surface ocean stratification and trophic conditions could be the causes of reduced abundance, diversity and species-specific changes in calcification in planktic foraminifera.

1. Introduction

The single-celled foraminifera comprise the most diverse group of calcareous plankton of the modern ocean. The majority of foraminifer species are benthic. About 50 morphospecies are planktic, which have a calcareous exoskeleton organized in chambers (i.e., d'Orbigny, 1826; Hemleben et al., 1989; Goldstein, 1999). The species from different environments can be characterized by differences in wall structure, pore size and spatial density, spines and test shape, which are partly related to adaptation. The distribution of foraminifera is thought to be influenced by food availability, temperature, salinity, turbidity, sunlight, and predatory presence; these factors provoke an overall water depth preference, which shifts during ontogeny, and seasonal preference for each species (Schiebel and Hemleben, 2005; Hemleben et al., 1989). Some of them are found only in the photic zone because they are symbiont-bearing and depend on light for photosynthesis. After reproduction, the empty shells sink to the seafloor, where their fossils are useful for paleoceanographic studies (e.g., Shackleton, 1968; Rohling et al., 2004; Mojtahid et al., 2015). Ecological tolerance limits of modern foraminifera are not completely defined, but progressive reduction in abundance (caused by worsening of their organic functions like food uptake, growth and reproduction, until death) is related with their departure from optimum conditions (Bé, 1977; Arnold and Parker, 1999). The absolute abundance of foraminifera is also affected by a predictable and distinct seasonal cycle for each species driven by the food source content of the watermass (Hemleben, 1989; Bé and Tolderlund, 1971; for Mediterranean examples see: Pujol and Vergraud-Grazzini, 1995; Bárcena et al., 2004; Hernández-Almeida et al., 2011; Rigual-Hernández et al., 2012; de Castro Coppa et al., 1980).

A vast majority of studies on planktic foraminifera are based on samples from bottom sediments and sediment cores, mainly for paleoceanographic purposes, with few studies considering the modern population in the water column, including the Mediterranean Sea. The first modern study of planktic foraminifera in this specific area was based on surface sediment samples collected by the Swedish Deep-Sea expedition of 1947-48 (Pettersson, 1953). A subsequent study found different species assemblages between the western basin, the eastern basin, and the Aegean Sea (Parker, 1955). The pioneering study of foraminifera population variability in the water column of the Mediterranean was conducted by Glaçon et al. (1971) in the Ligurian Sea, showing large seasonal variations of the relative abundances of the different species. Such variations of planktic foraminiferal assemblages in the water column were also reported for the Bay of Naples (de Castro Coppa et al., 1980). Cifelli (1974) was the first to cover the broader Mediterranean, with plankton tows of the upper 250m of the water column from west Madeira to the Isle of Rhodes in June 1969; they identified prominent differenced relative abundances of subtropical and subpolar species in different parts of the Mediterranean.

Thunell (1978) studied the upper 2 cm of sediment cores retrieved in different sites of the Mediterranean Sea and concluded that the distribution of planktic foraminifera was closely related to the distribution of the different surface water masses. There are specific temperature and salinity ranges for each water mass, as Bé and Tolderlund (1971) stated for the Atlantic, and a partial isolation effect in the different basins and sub-basins of the Mediterranean. Those hydrographis differences result in different species assemblages in each region. This contradicts somewhat with Pujol and Vergraud-Grazzini (1995), who gained quantitative data with flow-metered plankton tows in the upper 350 m of the water column, through a NW-SE Mediterranean transect from September-October 1986 and February 1988, and the

Alboran Sea in April 1990. They concluded that despite the W-E temperature and salinity gradients observed, those were not large enough and no close correlation was found to justify the extremely variable foraminifera assemblages, with high seasonal and geographical variations in absolute and relative abundances. They suggested that food availability is the main factor controlling their seasonal and geographical distribution and abundance; and when nutrients are sufficient, hydrographic structures like eddies and fronts play the main role.

Despite no new plankton tow study being carried out in the entire Mediterranean Sea, three regional studies based on sediment traps were realized in the Alboran Sea (Bárcena et al., 2004; Hernández-Almeida et al., 2011) and the Gulf of Lion (Rigual-Hernández et al., 2012). The one-year time series of the Alboran Sea sediment traps (July 1997 – May 1998) showed big differences in the main species distribution and daily fluxes, driven by food availability (related with water mixing/stratification periods) and temperature (Bárcena et al., 2004; Hernández-Almeida et al., 2011). The 12-year sediment trap records in the Gulf of Lion (October 1993 – January 2006) showed a strong seasonal pattern of the species, with more than 80% of the abundances from winter and spring in correlation with the nutrient supply and mixed water column conditions (Rigual-Hernández et al., 2012).

The calcification of foraminifera is affected by the chemical state of their surrounding waters. Theoretically, their shell mass is positively related to temperature, pH, $[Ca^{2+}]$, alkalinity and $[CO_3^{2-}]$ and negatively related to the $[CO_2]$ of the surrounding waters (Schiebel and Hemleben, 2005). Different studies conducted on water column foraminifera show differential results, as their shell mass can either be positively (Aldridge et al., 2012; Beer et al., 2010a; Marshall et al., 2013; Moy et al., 2009) but also negatively related to $[CO_2]$ (Beer et al. 2010a). Also, other studies report a positive effect of the temperature on foraminifera shell mass (Mohan et al. 2015; Aldridge et al., 2012; Marshall et al., 2013; Weinkauf et al., 2016). Beer et al. (2010a) suggest a species-specific relation between shell mass and $[CO_3^{-2}]$, depending on the presence or absence of symbionts. Some authors suggest that other factors like ecological stress do not affect the calcification intensity (Weinkauf et al., 2013). For further studies that relate foraminiferal calcification with environmental parameters see Weinkauf et al. (2016); Table 7. From the onset of the industrial era, anthropogenic emissions of CO_2 have led to ocean acidification, decreasing seawater pH and $[CO_3^{2-}]$, which provokes reduced stability of $CaCO_3$ that may reduce the formation of foraminiferal tests (Zeebe, 2012; de Moel et al., 2009; Moy et al., 2009).

Studies of the ecology of foraminifera in the Mediterranean waters remain scarce. Few studies exist covering the entire Mediterranean Sea; most are focused on specific regions, i.e., the Gulf of Naples (de Castro Coppa et al., 1980), the Alboran Sea plus the southwestern Mediterranean (van Raden et al., 2011). Data on living planktic foraminiferal abundances were provided by Cifelli (1974; spring only) and more recently by Pujol and Vergraud-Grazzini (1995). In addition, few size-normalized weight (SNW) and area density (ρ_A) studies from water column foraminifera are available in the literature (see Schiebel et al., 2007; Beer et al., 2010a; Aldridge et al., 2012; Marshall et al., 2013; Mohan et al., 2015; Marshall et al., 2015; Weinkauf et al., 2016)..New data are needed, since environmental conditions of the water column and associated foraminiferal assemblages might have changed over the past 20 years.

111 In this study, new quantitative and qualitative data are presented on living planktic foraminifera, across
112 the Mediterranean Sea during spring2013. Comparisons are made with previous studies from Pujol and
113 Vergraud-Grazzini (1995), Cifelli (1974), de Castro Coppa et al. (1980), Bárcena et al. (2004),
114 Hernández-Almeida et al. (2011), Rigual-Hernández et al. (2012) and Thunell (1978). The study by
115 Thunell (1978) is based on surface sediments, which can provide information, but might be biased
116 towards faster-sinking and more hydrodynamic tests due to shorter exposure to dissolution processes
117 (Caromel et. al., 2014; Schiebel et al., 2007), and towards tests with thicker walls that are better preserved
118 (Thunell, 1978). Although core top samples (0-2 cm) are suitable to infer modern variability (Thunell;
119 1978), they can cover the last few decades to few centuries, depending on the sedimentation rate, while
120 our plankton tow sampling represents a relative "snap shot" (Mortyn and Charles, 2003). In addition,
121 empty tests are passive particles that ocean currents may displace horizontally, but that displacement is
122 negligible due to their quick settling velocities (Caromel et al., 2014). Correlated results between plankton
123 tows (Pujol and Vergraud-Grazzini, 1995) and surface sediments (Vergraud-Grazzini et al., 1986) at
124 coincident places in the Mediterranean confirm the results obtained by Thunell (1978).

125 The objectives here are to (1) delineate new absolute abundances of planktic foraminifera within the
126 different regions of the Mediterranean Sea during spring, (2) characterize, at the species level their
127 ecology through their seasonal and geographical distribution and abundance by comparison with previous
128 studies, and (3) provide new ρ_A data for comparisons between basins and with other studies in the context
129 of ocean warming and acidification over the past 20 to 40 years.

130

131 ## 2. Oceanographic Setting

132 The Mediterranean Sea, with a strong thermohaline and wind-driven circulation, and a surface of
133 approximately 2,500,000 km^2, is divided into two main basins near the Strait of Sicily: the western and
134 eastern basins. These basins are composed of different sub-basins due to partial isolation caused by sills
135 that influence the water circulation, and by different water properties (Rohling et al., 2015; Rohling et al.,
136 2009). Natural connection with the ocean is through the narrow Strait of Gibraltar, where nutrient-rich
137 Atlantic surface waters enter the Mediterranean and experience an eastward increase of temperature and
138 salinity (Fig. 1) driven by insolation and evaporation, having a negative hydrological balance
139 (evaporation exceeding precipitation). The Mediterranean becomes increasingly oligotrophic towards the
140 east (Fig. 1; Fig. 2). In addition, the incoming Atlantic waters enter the Algero–Provençal Basin as far as
141 the Tyrrhenian Sea, and contribute to deep water formation in the Gulf of Lion in cold winters (Rohling et
142 al., 2015; Rohling et al., 2009).

143 In the eastern basin, two main sources of deep-water formation are active mainly during winter in the
144 Adriatic and the Aegean Seas. Cold dry winds cause evaporation and cooling forming denser and more
145 saline water masses that sink to depth (Rohling et al., 2015; Rohling et al., 2009; Hassoun et al., 2015b).
146 The same process is active in the Levantine basin, forming an intermediate water mass, which become
147 progressively cooler and fresher toward the western basin. Some waters reach the Tyrrhenian Sea. Waters
148 returning to the Atlantic through the Strait of Gibraltar at depth are cooler and saltier than the inbound

waters, and compensate for the inflow from the Atlantic. The Mediterranean Sea has a large physicochemical gradient for such a small marginal sea (Rohling et al., 2015; Rohling et al., 2009; Fig. 1).

3. Methodology

3. 1. Study Area

Plankton tow samples were collected during the MedSeA (Mediterranean Sea Acidification in a Changing Climate) cruise from 02 May to 02 June 2013 on board the Spanish R/V *Ángeles Alvariño*. The transect was divided into two legs (Fig. 2). The first leg ranged from the Atlantic Ocean near the Gibraltar Strait (adjacent to Cadiz Harbour, Spain) until the Levantine sub-basin in the Eastern Mediterranean (3879 km long, 11 sampling sites). The second leg started in Heraklion, Crete (Greece) into the Ionian Sea, south of the Adriatic and Tyrrhenian Seas and finished in the North Algero-Provençal basin, adjacent to Barcelona, Spain (3232 km long, 9 sampling sites, Fig. 2).

3. 2. Material and methods

Twenty samples were collected with BONGO nets (mesh size 150 µm and 40 cm diameter, for further details see Posgay, 1980) primarily 200 m depth, but also including tow time integrating the upper water column from 200m to the surface (Table 1). The sampling device was equipped with a flow-meter allowing the estimation of the volume filtered in each tow. The data for temperature, salinity, oxygen and fluorescence were integrated over the upper 200m from the nearest CTD stations retrieved during the same cruise (for the complete dataset see Ziveri and Grelaud, 2015). Seawater carbonate data (total alkalinity (AT), and dissolved inorganic carbon (DIC)) were obtained from water samples retirieved at various depths during the CTD casts (see Goyet et al., 2015). These data were used to calculate pH, pCO_2, and $[CO_3^{2-}]$ using the software CO2Sys (Lewis and Wallace, 1998) with the equilibrium constants of Mehrbach (1973) refitted by Dickson and Millero (1987). These three parameters of the carbonate system were then integrated for the upper 200m. The nutrient concentrations ($[PO_4]$ and $[NO_3]$) were measured by OGS (Italaian National Institute of Oceanography and Experimental Geophysics). The water samples were filtered on glass fiber filters (Whatman GF/F; 0.7 µm) and then kept at -20ºC onboard. The samples were then analyzed in laboratory with a Bran+Luebbe3 AutoAnalyzer (see Grasshoff et al., 1999). Surface chlorophyll *a* concentration was obtained from MODIS Aqua L2 satellite (NASA Goddard Space Flight Center: http://oceandata.sci.gsfc.nasa.gov/).

Foraminiferal samples were collected either at daytime or nighttime. Plankton samples were preserved by adding a 4 % formaldehyde solution buffered with hexamethyltetramine at pH = 8.2 on board. Individuals were not necessarily alive when collected and no distinction was made between cytoplasm-bearing tests: as alive or dead but still containing cytoplasm (see also Boltovskoy and Lena, 1970) and empty tests

(dead) were considered for this study. From each sampling station, the foraminifera were isolated and identified at species level. Samples were studied from the collecting bottles and the bottom collector, the latter representing 52.33 % of the total sample were treated in aliquots of 1/2, 1/4, 1/6, until 1/8. For each sample, each species was counted and isolated according to 3 size fractions (150–350 μm, ≥350–500 μm, and >500 μm) to determine the absolute and relative abundances. Foraminifera smaller than 150 μm, with tests partially broken and/or with organic matter attached were discarded.

We classified the different foraminifera species by visual identification under optical microscopy. Following the morphometric guidelines and taxonomic nomenclature proposed by Aurahs et al. (2011) for *Globigerinoides ruber* (white), *Globigerinoides ruber* (pink) and *Globigerinoides elongatus*. For *Trilobatus sacculifer* (with sac) and *T. sacculifer* (without sac) we used Spezzaferri et al. (2015). Hemleben et al. (1989) was used as a guide to classify *Globigerina bulloides, Orbulina universa, Globorotalia inflata, Globorotalia menardii*, and *Hastigerina pelagica*. *Globigerinoides quadrilobatus* was inferred from Papp and Schmid (1985). *G.bulloides* could not be differentiated from *Globigerina falconensis* in our samples and are treated together; the *G. bulloides/G. falconensis* plexus is referred to as *G. bulloides* in our study. *Globigerinella siphonifera/G. calida/ G. radians* plexus (see Weiner et al., 2015) is treated as *G. siphonifera* in our study.

For the area density (ρ_A) study, we selected three main species: *G. ruber*, *G. bulloides* and *O. universa*. All specimens of these three species were photographed with a *Canon EOS 650 D* camera device attached to a *Leica Z16 AP0* microscope to measure their long axis and silhouette area using the software ImageJ (Schneider et al., 2012). For each station and each of the three selected species, the individuals were weighed together by triplicate with a Mettler Toledo XS3DU microbalance (±1 μg of nominal precision) within 50 μm size fraction increments (150-200 μm, 200-250 μm, etc.). Cytoplasm-filled or empty dry-weighed foraminifera tests were weighted together since dry cytoplasm has no statistically significant effect on the weight of tests >150 μm (Schiebel et al., 2007). Specimens containing notable organic matter attached to the test were discarded. The maximum number of individuals weighed together was 5; in some stations individuals were measured individually as no more specimens were available. In all the cases the mean weight per specimen of the three weightings was applied. The silhouette area obtained was then used to measure the ρ_A (Marshall et al., 2013; Marshall et al., 2015).

3.3. Statistical methods

We performed a principal component analysis (PCA; Varimax rotation) using SPSS Statistic 23 software. The PCA was performed on the environmental parameters: temperature, salinity, oxygen, fluorescence, NO_3, PO_4, pH, pCO_2, and $[CO_3^{-2}]$, from every station. Two components, which together explain 77 % of the total variance, were obtained (Fig. 7): The first factor exhibited positive loadings on the nutrients and the fluorescence and negative loadings on temperature and salinity (and to a lesser degree on $[CO_3^{2-}]$). This factor explains 56.99% of the total variance and represents the strong west-east gradient characterizing the Mediterranean Sea as the water becomes warmer, saltier and more oligotrophic eastwards. The second factor explains about 20.02% of the total variance and is characterized by positive loadings on pH and oxygen concentrations (and to a lesser degree on $[CO_3^{-2}]$) and a negative loading on

224 the pCO_2. It is interpreted as the variations of the carbonate system properties in the Mediterranean Sea
225 with slightly lower surface water pH in the western basin compared to the eastern basin. The sample
226 scores on the first 2 factors with overlay of absolute abundances of foraminifera species (*G. ruber*
227 (white), *G. bulloides*, *G. inflata*, *O. universa* and *T. sacculifer* (without sac)) and area density (*G. ruber*
228 (white), *G. bulloides* and *O. universa*) are shown in Figure 7).

229

230 ## 4. Results

231

232 ### 4. 1. Absolute and relative abundance

233 The absolute abundance of planktic foraminifera collected with BONGO nets has a mean value of 1.42
234 ±1.43(SD) individuals·10 m^{-3}. A maximum value of 5.2 ind.·10 m^{-3} in the Strait of Gibraltar is followed
235 by 4.14 ind.·10 m^{-3} in the Alboran Sea, 3.61 ind.·10 m^{-3} in the Tyrrhenian Sea, and 3.00 ind.·10 m^{-3} off
236 southern Crete (Fig. 3; Fig. 7a). With the exception of these four regions, a standing stock of 1.7 ind.·10
237 m^{-3} is not surpassed in any other station. A minimum standing stock occurs in the Adriatic Sea (0.11
238 ind.·10 m^{-3}). The westernmost stations (2 and 3) with the highest Atlantic influence have the highest
239 abundance values (4.67 ind.·10 m^{-3} on average), followed by the eastern Mediterranean Stations 9 to 13
240 (1.31 ind.·10 m^{-3}), and the western Mediterranean (Stations 5, 6, 20, 21 and 22; 0.77 ind.·10 m^{-3}) with a
241 clearer difference within the southwest (Stations 5 and 6; 1.08 ind.·10 m^{-3}) and the northwest (Stations 20
242 to 22; 0.56 ind.·10 m^{-3}; Fig. 3; Fig. 7a; Appendix A). Pervasively, the most common size fraction of
243 foraminifera is 150–350 µm (65.57%; Fig. 4), especially due to the contribution of *G. ruber* (white) and
244 *G. bulloides*. The exceptions are at Station 3 with a high presence of 350–500-µm sized *G. inflata*, and
245 Station 7a mainly due to >500-µm sized *O. universa*, and 350–500-µm sized *G. siphonifera* and *G.*
246 *inflata.* The 350-500-µm size fraction dominates in the western Mediterranean and is progressively
247 reduced eastwards (Fig. 4), mainly due to the contribution of small *G. inflata* from the 150-350 µm size
248 fraction. Overall,higher percentages of individuals >500 µm are found in the western part of the
249 Mediterranean compared to the eastern part (Fig. 4). The highest percentages are found at the Strait of
250 Sicily and the Northern Ionian Sea (St. 7a, 16-18; Fig. 4; Fig. S1; Appendix A). However, due to the
251 extremely low standing stocks the above observations are mere snapshots, and may not be generalized.

252 The most abundant species is *G. ruber* (white) (with an average of 0.30 ind.·10 m^{-3}, representing 21.49%
253 of the total assemblage); its highest abundances are found in the Tyrrhenian Sea (1.69 ind.·10 m^{-3}) and in
254 the eastern Mediterranean (Stations 10 and 13). It is not present in the Adriatic Sea, at Station 16–18, and
255 in the northwestern Mediterranean. It is found in low numbers in the southwestern Mediterranean,
256 Atlantic, and Strait of Gibraltar stations (Fig. 3; Fig. 7d). Individuals >350 µm in test long axis are rare
257 (Appendix A). *G. inflata* is the second most abundant species (0.29 ind.·10 m^{-3}; 20.19%), mainly due to
258 its high abundance in the Alboran Sea (3.5 ind.·10 m^{-3}; 61.08% of the sample). It is present in the western
259 Mediterranean until the Strait of Sicily. East of the Strait of Sicily, it is only found with low abundances
260 at the westernmost stations (Fig. 3; Fig. 7b). The dominant size fraction is 350-500 µm (Appendix A). *G.*
261 *bulloides* has an average abundance of 0.24 ind.·10 m^{-3} (17.20 %), mainly due to its abundance in the

Strait of Gibraltar (2.31 ind.·10 m^{-3}; 47.34 %). It is slightly more abundant in the southwestern Mediterranean and the Tyrrhenian Sea. It is a quite ubiquitous species being absent at four stations (Fig. 3; Fig. 7e). It rarely appears in the >350-µm test-size fraction (Appendix A).

Trilobus sacculifer (without sac; also referred as *T. trilobus*; on average 0.13 ind.·10 m^{-3}; 9.16 %), is especially notable at the Strait of Gibraltar (50.91 %; Fig. 3; Fig. 7c). *O. universa* is ubiquitous in the whole Mediterranean Sea with the exception of the three Stations 6, 9, and 14 (Fig. 3; Fig. 7f). Its average abundance is 0.12 ind.·10 m^{-3} (8.70 %). Its dominant size fractions are ≥350 µm (Appendix A; Fig. 4). *G. elongatus* (0.09 ind.·10 m^{-3}; 6.41 %) is found mostly at the same stations as *G. ruber* (white), but is usually less abundant (Fig. 3). It is most frequent in the ≥350-500-µm test-size fraction, and some individuals >500 µm are found in the Atlantic (Appendix A). The other species appear in very low numbers: *G. quadrilobatus* (0.07 ind.·10 m^{-3}), *G. siphonifera* (0.03 ind.·10 m^{-3}), *G. ruber* (pink) (0.02 ind.·10 m^{-3}), *H. pelagica* (0.008 ind.·10 m^{-3}), *G. menardii* (0.001 ind.·10 m^{-3}) and *T. sacculifer* (with sac) (0.001 ind.·10 m^{-3}; Fig. 3; Appendix A).The PCA performed on the environmental parameters and the sample scores on the two first components clearly shows a separation, regarding Factor 1, between the western and eastern Mediterranean stations (Fig. 7). The western basin, which is characterized by more food availability for the foraminifera, lower temperature and lower salinity, is where the absolute abundances are the highest (Fig. 7a). In the eastern basin, station 10 is an exception with a considerable contribution from *G. ruber* (white) to the absolute abundances (Fig. 7a). Regarding Factor 2, the stations more influenced by the incoming waters from the Atlantic have the lowest [CO_3^{-2}] values. The stations where absolute abundances show some affinity for more "acidic" conditions are in the NW Mediterranean, the Tyrrhenian Sea, and in the northern Ionian Sea (stations 14, 15 and 16). The majority of the Ionian Sea stations and all the Levantine Basin stations show average values (Fig. 7a). Overall, the highest absolute abundance of all foraminifera seems related to food availability and only secondarily to the carbonate system (Fig. 7a).

With the exception of the Tyrrhenian Sea, *G. ruber* (white) abundance is positively correlated with warmer and saltier waters, and lower pH (Fig. 7d). The opposite is observed for *G. bulloides*, higher abundances occur where more food is availabile and at stations where pH is higher (Fig. 7e). *O. universa* shows an ubiquitous distribution with no remarkable trends within the two factors (Fig. 7f). The irregular abundance distribution of *T. sacculifer* (without sac) does not folow any remarkable trend (Fig. 7c). *G. inflata* positively correlates with food availability, and the regional distribution follows the path of Atlantic waters (Fig. 7b).

To show the relative abundance of the various species, some stations were grouped together to achieve a minimum number of foraminifera (>95 tests); the grouping was set by location proximity in which foraminiferal assemblages were similar. The stations at the Strait of Sicily and the western Mediterranean (Stations 20, 21, 22) are not shown due to a low number of individuals (< 90; Fig. 5). Some similarities can be seen between the Tyrrhenian Sea and the eastern Mediterranean, and also between the Alboran Sea and the southwestern Mediterranean. The Atlantic and the Ionian–Adriatic–Aegean grouping have similar proportions of species. On the other hand, the Tyrrhenian Sea and the eastern Mediterranean stations were dominated by *G. ruber* (white), the Alboran Sea by *G. inflata*. The dominance of a single species in the

301 southwestern Mediterranean is less clear, which might be due to low numbers of individuals (*G.inflata*
302 being the main species followed by *G. bulloides* as in the Alboran Sea station). *T. sacculifer* (without sac)
303 has a high relative abundance in the Atlantic Ocean and in the Strait of Gibraltar, being the main and the
304 second most abundant species, respectively. At all other stations analyzed, *T. sacculifer* (without sac) is
305 less abundant. *G. bulloides* is most frequent in the entire western Basin and the Atlantic Ocean, being the
306 main species in the Strait of Gibraltar. It is less frequent in the Tyrrhenian Sea, and in the eastern Basin
307 and its sub-basins. *G. bulloides* contrasts with *G. ruber* (white), which always represents a small
308 percentage in the western Mediterranean but dominates the Tyrrhenian Sea and the eastern Basin (Fig. 5;
309 Appendix A).

310

311 **4. 2. Area density (ρ_A)**

312 Due to their abundance, *G. ruber* (white), *G. bulloides*, and *O. universa* were analyzed for their area
313 density (ρ_A; Fig. 6; Fig. 7g-i). The high two-dimensional (silhouette) area-to-long axis correlation is best
314 fitted by a power regression (Fig. S2). The same growth pattern can be seen in *G. ruber* (white), *G.*
315 *bulloides*, and *O. universa* with that correlation, represented graphically in the shape of a power function
316 (Fig. S2). They grow slightly faster when they are younger and smaller (steepest in the lower left part of
317 the regression line) and slightly slower when they grow older and bigger (less steep in the upper right part
318 of the regression line; Fig. S2). The specimens of *G. ruber* (white) from the Atlantic have the largest size
319 followed by individuals from the Tyrrhenian Sea, and those from the eastern Ionian Sea. For the other two
320 species *G. bulloides* and *O. universa*, a similar trend is observed regarding the two basins, with the
321 eastern Mediterranean having the smallest individuals, while the largest individuals occurred in the
322 Atlantic and the northwestern Mediterranean (Fig. S2). The different locations were grouped using the
323 same criteria as in Fig. 5.

324 The long axis-to-weight relation of *G. ruber* (white) specimens yielded an $r^2 = 0.841$ (linear regression
325 throughout this paragraph; Fig. S3), followed by *O. universa* ($r^2 = 0.63$), and *G. bulloides* ($r^2 = 0.516$; Fig.
326 S3). *O. universa* was finally discarded for comparisons between ρ_A at different locations due to a low
327 area-weight correlation and no remarkable trend observable between locations (Fig. S4c; Fig. 7i); while
328 data from *G. ruber* (white) correlate well (Fig. S4a). The eastern Mediterranean specimens are the lightest
329 for both species (*G. ruber* (white), *G. bulloides*), with more extreme W-E differences for *G. ruber* (white)
330 (Fig. S4d-e).

331 The ρ_A of *G. ruber* (white) specimens from six locations were compared (Fig. 6). The eastern
332 Mediterranean individuals have the lowest median ρ_A (approximately between $7.5 \cdot 10^{-5}$ and $9 \cdot 10^{-5}$ $\mu g \cdot \mu m^{-2}$), with lower values eastward, and a small interquartile range ($IQR = Q_3 - Q_1$). The Atlantic individuals
334 of *G. ruber* (white) show the highest median value ($1.55 \cdot 10^{-4}$ $\mu g \cdot \mu m^{-2}$) and IQR. The ρ_A of Tyrrhenian
335 individuals ranges between those from the eastern Mediterranean and Atlantic Ocean ($1.2 \cdot 10^{-4}$ $\mu g \cdot \mu m^{-2}$).
336 The ρ_A of *G. ruber* (white) for each station was compared with the two PCA factors; higher ρ_A are related
337 to slightly lower pH and higher food availability in the western Mediterranean and Atlantic stations (Fig.
338 7g).

For *G. bulloides* specimens, seven locations were compared (Fig. 6). The Atlantic has the lowest median ρ_A ($8.75 \cdot 10^{-5}$ $\mu g \cdot \mu m^{-2}$) and the smallest IQR, showing an opposite trend as in *G. ruber* (white). Also contrary to *G. ruber* (white), *G. bulloides* from the eastern Mediterranean tend to have a higher median ρ_A ($9.75 \cdot 10^{-5}$ $\mu g \cdot \mu m^{-2}$) and a larger IQR. The differences in ρ_A between the eastern and western Mediterranean are smaller in *G. bulloides* than in *G. ruber* (white). The ρ_A of *G. bulloides* at each station was compared with the two PCA factors. Results show a less clear overall trend for *G. bulloides* than for *G. ruber* (white), with the higher ρ_A associated with slightly higher pH in the eastern Mediterranean sea-water (Fig. 7h).

5. Discussion

5. 1. Abundance and diversity patterns

Absolute abundance values of 4.2 individuals per 10 m^{-3} (≥150 μm) on average are low in comparison with other water column foraminifera studies, even for oligotrophic regions. For example, in the oligotrophic northern Red Sea, less than 100 ind.·10 m^{-3} (>125 μm) were reported from surface waters, and standing stocks were much higher than 100 ind.·10 m^{-3} at most of the sites sampled in 1984 and 1985 (Auras-Schudnagies et al., 1989). In the oligotrophic to mesotrophic Caribbean and Sargasso Seas, standing stocks were up to 786 ind.·10 m^{-3} (>100 μm) and 907 ind.·10 m^{-3} (>202 μm), respectively (Schmuker and Schiebel, 2002, and references therein). In theAtlantic, south of the Azores Islands, Schiebel et al. (2002) counted an average of 66.15 ind.·10 m^{-3} for the upper 100 m in August 1997, and 422.97 ind.·10 m^{-3} in January 1999 (>100 μm). Other similar studies show higher abundances of one or two orders of magnitude (i.e. Sousa et al., 2014; Boltovskoy et al., 2000; Kuroyanagi and Kawahata, 2004; Rao et al., 1991; Ottens, 1992; Schiebel et al., 1995). At higher latitudes, in the Fram Strait (Arctic Ocean), Pados and Spielhagen (2014) obtained approximate values of 117 ind.·10 m^{-3} from the upper 500 m in late June-early July of 2011. Mortyn and Charles (2003), in February-March 1996, at 200 m depth range in the Atlantic sector of the Southern Ocean, found as a minimum value 0.1 ind.·10 m^{-3}, with an approximate mean of 73 ind.·10 m^{-3}.

Within the Mediterranean, a previous study with results comparable to ours, sampled the upper 350 m (Pujol and Vergraud-Grazzini, 1995). For the Alboran Sea, samples were obtained during a similar period of the year (April 1990) with values around 16, 6 and 9 ind.·10 m^{-3}, greater than in the Station 3 (4.14 ind.·10 m^{-3}). Samples from different seasons have higher abundances, with highest values in February (Pujol and Vergraud-Grazzini, 1995), and a high annual average of 9.3 ind.·10 m^{-3}. Regarding Pujol and Vergraud-Grazzini (1995), western Mediterranean abundances are higher than the eastern ones, due to more oligotrophic conditions and higher temperature and salinities in the east that limit foraminiferal

374 production during winter and late summer. In concordance with Pujol and Vergraud-Grazzini (1995), no
375 differences are observed between samples collected during day and night.

376 Comparing with previous studies that covered the Mediterranean, we notice that Thunell (1978) and Pujol
377 and Vergraud-Grazzini (1995) did not find *G. menardii*, while it was reported by Cifelli (1974) in very
378 low abundances. The fact that *G. menardii*, which has a preference for tropical waters, is not found in the
379 surface sediments suggests that it is a new species in the Mediterranean Sea (Cifelli, 1974). Its recent
380 presence in the Mediterranean Sea could be related to the warming of the waters. All other species found
381 in our study were also found in the past studies covering the Mediterranean Sea (Cifelli, 1974; Thunell,
382 1978; Pujol and Vergraud-Grazzini, 1995). It remains unclear whether Pujol and Vergraud-Grazzini
383 (1998) found *G. falconensis* and classified it with *G. bulloides*, or if Thunell (1978) found *G. elongatus*
384 and *T. sacculifer* (without sac) and classified them as *G. ruber* and *G. sacculifer*, respectively. Also, it is
385 not certain if Cifelli (1974) found *G. calida* and classified it with *G. aequilateralis* (older synonym of *G.*
386 *siphonifera*). From the figures in Cifelli (1974), we suspect that *G. elongatus* was classified as *G. ruber*.
387 In the same way, we do not find any evidence of *T. sacculifer* (with sac) from the figures presented by
388 Cifelli (1974), but we cannot discard the possibility that this species was classified as *Globigerinoides*
389 *trilobus* (*T. sacculifer* without sac).
390
391 *Globigerinoides quadrilobatus* was not found in any previous plankton tow studies in the Mediterranean,
392 but is abundant in sedimentary cores (i.e. Cramp et al., 1988; Rio et al., 1990); there exists the possibility
393 to classify it with *G. sacculifer* or *G. trilobus* in previous studies as suggested by Hemleben et al. (1989).
394 Some species, which are absent from our samples, reached high frequencies in the aforementioned
395 studies, i.e., *Turborotalita quinqueloba*, *Neogloboquadrina pachyderma*, and *Globorotalia*
396 *truncatulinoides*. The fact that these species were not sampled in the present study may be due to their
397 absence or presence at extremely low abundances of adult specimens at the sampled stations in May, as
398 they present generally low abundances in spring according to a 12-year sediment trap record in the Gulf
399 of Lion (Rigual-Hernández et al., 2012). Another possibility is their presence in test sizes smaller than
400 150 μm, which is smaller than the mesh size of our BONGO nets, a possibility potentially supported by
401 previous Mediterranean studies using smallesr mesh sizes (see Pujol and Vergraud-Grazzini, 1998, 120
402 μm mesh size; Rigual-Hernández et al., 2012, 63-150 μm mesh size).
403
404 To propose a quantitative comparison of the number of species found in previous studies in the
405 Mediterranean, we used the morphospecies identified in them by the authors of each study. We identified
406 12 morphospecies, clearly less than Cifelli (1974), Thunell (1978) and Pujol and Vergraud-Grazzini
407 (1995), with 18 morphospecies in total. At Station 3 of this study (Alboran Sea), we found 8
408 morphospecies; whereas Rigual-Hernández et al. (2012) found 12 morphospecies during the same season.
409 The lower absolute abundance of individuals in our study compared to Pujol and Vergraud-Grazzini
410 (1995), together with low species diversity in the Mediterranean, may indicate a trend of changing
411 conditions over the last decades, as it has been reported for temperature and salinity (Yáñez et al., 2010),
412 alkalinity (Cossarini et al., 2015; Hassoun et al., 2015a), and water mass mixing (Hassoun et al., 2015b).
413 These changing conditions could also imply changes in the ecology and distribution of planktic

foraminifera, as discussed below. Note that our mesh size is larger than that of Pujol and Vergraud-Grazzini (1995) and Rigual-Hernández et al. (2012), but is similar to that of Cifelli (1974): mesh size of 158 μm. A larger mesh size would explain the lower numbers in absolute abundance and reduced diversity, but the higher diversity observed by Cifelli (1974) in June supports our idea of changing ecological conditions.

The western part of the first transect (from the Atlantic to the Strait of Sicily) has a higher percentage of larger size fractions than the eastern part. The main cause of the increase in test size is a change in species composition. For example, large sized *G. inflata* (especially in the 350-500 μm fraction) are present with higher abundances in the west than in the east. The same is true for the presence of large *O. universa* (especially in the >500 μm), plus the contribution of *G. siphonifera*, which is larger in stations where it is more frequent (Appendix A; Fig. 4).

5. 2. Factors controlling the abundance of the main species

This discussion focuses on the five main species of our samples. The spinose and symbiont-bearing species: *G. ruber* (white), *O. universa*, and *T. sacculifer* (without sac), which mainly inhabit tropical and subtropical waters. *G. ruber* (white) is the main species in the Atlantic. *O. universa* is rather ubiquitous, also being present in warm transitional Atlantic waters (Bé and Tolderlund, 1971). The spinose and nonsymbiotic species *G. bulloides*, is typical of subpolar and transitional regions as well as upwelling areas, and is also found in subtropical and tropical waters at a much lower abundances, characterized by its wide temperature range (Thunell, 1978; Bé and Tolderlund, 1971). The non-spinose species *G. inflata* is typical of the temperate Atlantic Ocean (Bé and Tolderlund, 1971).

5. 2. 1. *Globigerinoides ruber* (white)

In our study, *G. ruber* (white) is found in the Atlantic with slightly higher absolute abundances and higher relative abundances than in the western Mediterranean Basin, where it is found in low abundances. Temperature-related factors may be the main cause, with warmer Atlantic waters (16.1 ºC) with respect to the western Mediterranean (14.3 ºC in the SW, 14.0 ºC in the NW; Fig. 1). These results are in agreement with the observations made by Cifelli (1974) in June 1969, where *G. ruber* (white) was by far more abundant in the eastern than the western Mediterranean Basin, being the most abundant species in the Levantine Basin and the south Ionian Sea; for these two locations it seems that *G. ruber* (white) is present independent of the seasons, winter included, which is also true for the pink variety (see also Thunell, 1978; Pujol and Vergraud-Grazzini, 1995). The increasing dominance of *G. ruber* (white) from the western to the eastern Mediterranean Basin coincides with the eastward increasing salinity (Fig. 7d). Its higher relative abundance in the eastern basin results from the ability of *G. ruber* to thrive in food-depleted conditions (Hemleben et al., 1989).

G. ruber (white) remains scarce or absent in May in the Ionian Sea stations (Fig. 3), increasing its abundance towards the Tyrrhenian Sea. On the other hand, in the Ionian Sea it exhibits relative abundance

451 below 60% in the surface sediments (Thunell, 1978), and decreases towards the Tyrrhenian Sea. This
452 situation could be due to higher food availability in the Tyrrhenian Sea in comparison to the Ionian Sea
453 during May 2013 (Fig. 1c; Fig. 7d) plus a small difference in temperature between both seas (Fig. 1a; Fig.
454 7d). This may not be the typical spring situation, as due to surface sediment evidence, the Ionian Sea
455 sediments are enriched in *G. ruber* tests (Thunell, 1978) and May is the most productive season in terms
456 of foraminiferal tests (Rigual-Hernández, 2012; Bárcena et al., 2004; Hernández-Almeida et al., 2011).
457 Also, we note that in May 1979, a scarce presence of *G. ruber* was reported in the Bay of Naples (de
458 Castro Coppa et al., 1980), whereas in our study *G. ruber* is present at 47 % in the Tyrrhenian Sea, being
459 the main species.

460 The dominance of *G. ruber* (white) and abundance peaks in May in the eastern Mediterranean (this
461 study), coincides with the positive temperature gradient between Station 9 and Station 13 (16.2–17.3 ºC;
462 Fig. 1). In late summer, *G. ruber* experiences its largest expansion and presence owing to warmer
463 temperatures and more oligotrophic conditions, clearly being the main species from the north of Algeria
464 to the Levantine Basin (Pujol and Vergraud-Grazzini, 1995). *G. ruber* (pink) is the dominant species at
465 the Strait of Sicily and eastwards (Pujol and Vergraud-Grazzini, 1995), whereas in May it only has
466 residual presence in some locations (especially around Crete; this study). In February, presumably due to
467 temperature decrease, *G. ruber* (pink) almost disappears from the Mediterranean and the other
468 morphotypes are present in low numbers (Pujol and Vergraud-Grazzini, 1995; Rigual-Hernández et al.,
469 2012), suggesting that *G. ruber* (white) and *G. elongatus* are better adapted to colder temperatures than
470 the pink variety. Hydrographic conditions and consequently food availability seem to be the limiting
471 factors for its abundance once it has reached its optimum temperature range.

472 5. 2. 2. *Globorotalia inflata*

473 The presence of *G. inflata* is related to cool waters and high food availability (Pujol and Vergraud-
474 Grazzini, 1995; Rigual-Hernández et al., 2012), following high phosphate concentrations (Ottens, 1992).
475 This explains its higher abundance in the cooler nutrient-rich western basin, and its progressive scarcity
476 toward the warmer oligotrophic eastern Mediterranean (Fig. 1; Cifelli, 1974; Thunell, 1978). The same
477 pattern is observed in late summer. From spring to late summer *G. inflata* shows a displacement from the
478 eastern Alboran Sea to the northwestern Mediterranean, decreasing frequency in the Algero–Provençal
479 Basin and the southwestern Mediterranean Basin, maintaining a residual presence in the eastern basin
480 (Pujol and Vergraud-Grazzini, 1995).In winter, with cooler temperatures, the opposite process happens,
481 and *G. inflata* becomes the dominant species in the Alboran Sea (Bárcena et al., 2004) and the
482 southwestern basin, with high frequencies in the Strait of Sicily and toward the Ionian Sea. Eastwards its
483 presence is maintained at only residual levels (Pujol and Vergraud-Grazzini, 1995). Its distribution along
484 the seasons shows that *G. inflata* is scarce or absent in warmer, stratified and nutrient-depleted regions of
485 the Mediterranean.

486 *G. inflata* is absent in the Tyrrhenian Sea, despite temperature ranges being comparable to those observed
487 in the southwestern Mediterranean, where this species is abundant (this study). In contrast, *G. inflata* was
488 reported in May 1979 in the Tyrrhenian Sea as the main species and became practically absent in the

warmer summer months (de Castro Coppa et al., 1980). *G. inflata* is reported in sediment trap data in the Gulf of Lion (Rigual-Hernández et al. (2012), close to our northwestern Mediterranean stations in which *G. inflata* is absent. In addition, the absolute abundances of *G. inflata* are closely related to the Factor 1 of the PCA, suggesting a certain affinity with food availability inferred from nutrients and fluorescence (see sample scores in Fig. 7b).We suggest that in the Mediterranean, food depletion plays a more important role in limiting its distribution than warm temperatures.

The spring distribution of *G. inflata*, with *G. bulloides* as a secondary species in the Alboran Sea matches with other studies (Pujol and Vergraud-Grazzini, 1995; van Raden et al., 2011). *G. inflata* peak abundances appear more to the west than those reported by Cifelli (1974) to the east of the Balearic Islands. Those peaks can be associated with nutrient-rich upwelling areas rich in foraminifer prey within its temperature range (Fig. 1; Fig. 2).

5. 2. 3. *Globigerina bulloides*

In accordance with Cifelli (1974), *G. bulloides* is the dominant species in the Atlantic station close to the Strait of Gibraltar, whereas in our study it shares dominance with other species (Station 1; Fig. 3). The *G. bulloides* dominance in the Strait of Gibraltar during late spring–early summer confirms the finding of Cifelli (1974). The abundance peak of *G. bulloides* in the Strait of Gibraltar (this study), coincides with high nutrient concentration and upwelling (Figs. 1, 2, and 3), making Station 2 the most rich in planktic foraminifera of all the transect. This confirms its association with upwelling, where phyto- and zooplanktonic blooms control its abundances, as it is an opportunistic species (Pujol and Vergraud-Grazzini, 1995; Sousa et al., 2014; Bárcena et al., 2004; Hernández-Almeida et al., 2011; Rigual-Hernández et al., 2012). It positively correlates with fluorescence peaks since it feeds on phytoplankton (Mortyn and Charles, 2003; Bárcena et al., 2004; Rigual-Hernández et al., 2012; Fig. 1).

In April (Pujol and Vergraud-Grazzini, 1995; van Raden et al., 2011) and May (this study), *G. bulloides* is found to be the second most abundant species, surpassed by *G. inflata*, in the westernmost Alboran Sea. High temperature anomalies provoke an inverse situation, thanks to faster *G. bulloides* reproduction plus *G. inflata* being further from its optimum temperature (Bárcena et al., 2004). One month later it is found to be the dominant species replacing *G. inflata*, which is still dominant in the eastern Alboran Sea (Cifelli, 1974). Its ubiquity and higher abundance in the western basin with respect to the east is supported by previous studies (i.e., Cifelli, 1974; Thunell, 1978), with a higher difference in abundance in February than in September–October (Pujol and Vergraud-Grazzini, 1995; Rigual-Hernández et al., 2012). In late summer, its presence is more secondary, with abundance peaks around the Strait of Sicily and south of Sardinia. Abundance peaks at the same locations plus the Gulf of Lion occur during winter, but with larger absolute abundances (Pujol and Vergraud-Grazzini, 1995; Rigual-Hernández et al., 2012).

G. bulloides decreases in abundance when food is depleted, observable in the eastern Mediterranean, where it always has lower absolute abundances than in the west, also in the summer months in the Gulf of Lion, when food is depleted and not renewed due to water stratification (Rigual-Hernández et al., 2012). During spring to late summer in the eastern basin, *G. bulloides* is less frequent, being more present just east of the Strait of Sicily (Cifelli, 1974; Pujol and Vergraud-Grazzini, 1995). During winter its

abundance increases and it becomes the second most abundant species in the Levantine Basin preceded by *G. ruber* (white), and it is also one of the main species in the Ionian Sea. Levantine waters have permanent eddies that sustain phytoplankton blooms, explaining the presence of *G. bulloides* in winter (Pujol and Vergraud-Grazzini, 1995). It is noticeable that northwards of the Levantine Basin and in the Aegean Sea its abundances are comparable to those in the western basin regarding surface sediment data from Thunell (1978).

G. bulloides has more affinity for cooler upwelled waters than warmer more stratified waters (Sousa et al., 2014; Thunell, 1978), being present in subtropical waters only in cooler months (Ottens, 1992). The coldest station of the first leg of this study (Strait of Gibraltar, 14.2 ºC) coincides with its abundance peak, and it is absent from the warmest station (off the Nile Delta, 17.6 ºC; Fig. 1a), which also is one of the most depleted in foraminiferal prey (Fig. 1c; Fig. 2). Its Its affinity for fresher and cooler waters matches with its low abundance in the eastern basin and its higher abundances in the western basin (northwestern basin included, despite its low absolute abundances but being the main species there; see also Rigual-Hernández et al., 2012), and with its seasonal distribution. Its presence and distribution seems to be limited by a combination of low nutrient concentration and limited food availability, caused by stratification of the surface water column, and increased sea surface temperatures.

5. 2. 4. *Orbulina universa*

Orbulina universa was found ubiquitous by Pujol and Vergraud-Grazzini (1995), being present in all the stations and seasons, reaching peak abundances in the southwestern Mediterranean both in late-summer and winter. Regarding our data, it follows the same pattern during spring, being absent from only three stations (St. 6, 9, and 14; Fig. 3; Fig. 7f). No abundance peak occurs in spring (our data) and in the report of Cifelli (1974), but abundances are slightly higher in the western basin to than the east. That small difference can be caused by more nutrient-rich upwelling areas (Sousa et al., 2014; Morard et al., 2013) in the western basin or by high salinities in the eastern basin.

5. 2. 5. *Trilobatus sacculifer* (without sac)

In June, *T. sacculifer* (without sac) is quite ubiquitous and represents 5 % of the assemblage in the Strait of Gibraltar (Cifelli, 1974). At our stations, *T. sacculifer* constituted up to 25 % of the assemblages in May, and was absent from seven stations (St. 5, 7a, 14, 15, 16-18, 20, 22). Lower percentages were found in April in the Alboran Sea (Pujol and Vergraud-Grazzini, 1995). In September–October *T. sacculifer* shows high abundances and is one of the main species from north of Minorca to the southwestern Mediterranean until the Strait of Sicily, where it is rare. In late summer it decreases considerably and progressively eastwards, where the highly dominant *G. ruber* is maintained as the most abundant species (Pujol and Vergraud-Grazzini, 1995), probably due to slightly higher temperature and salinity tolerance (see also Bijma et al., 1990). On the other hand, in February *T. sacculifer* (without sac) disappears from the north Levantine Basin and its abundances lowers considerably, being a residual species in terms of relative abundance in all the Mediterranean (Pujol and Vergraud-Grazzini, 1995).

564

565 **5. 3. Factors controlling planktic foraminiferal test weight**

566 The area density (ρ_A) of tests of both *G. ruber* (white) and *G. bulloides* follow a systematic change from
567 the Atlantic towards the eastern Mediterranean (Fig. 6). Therefore, the ρ_A of these two species is
568 interpreted and discussed for possible environmental effects and biological prerequisites in the following.
569 In contrast, the ρ_A of *O. universa* does not show any change between the western and eastern basins (Fig.
570 7i), and cannot be used to identify and quantify particular environmental effects.

571 5.3.1 Unknown control of the ρ_A of *O. universa*

572 No systematic change between the western and eastern basins in the ρ_A data of *O. universa* could be
573 explained by an insufficient understanding of the ecology of the different morphotypes and genotypes of
574 *O. universa*. Only one out of three genotypes (i.e. Type III, after Darling and Wade, 2008) is recorded in
575 the Mediterranean Sea (Mediterranean species, after de Vargas et al., 1999), The Mediterranean Type III
576 has been found to include two sub-types, Type IIIa and Type IIIb (André et al., 2014). The different
577 genotypes and morphotypes of *O. universa* tolerate wide ranges of salinity and temperature in surface
578 waters (i.e., de Vargas et al., 1999). Whereas the various types of *O. universa* differ in the pore-size (de
579 Vargas et al., 1999; Morard et al., 2009; Marshall et al., 2015), their pore-size is also affected by
580 environmental conditions including water temperature (i.e., Bé et al., 1973). Likewise, thickness of the
581 test wall has been described to vary between types (de Vargas et al., 1999; Morard et al., 2009; Marshall
582 et al., 2015), and is as well affected by environmental conditions and ontogenetic stage of specimens.
583 Adult *O. universa* have been shown to continuously add calcite layers to the proximal surface of the same
584 sphere (Spero, 1988; Spero et al., 2015). Since environmental and biological factors may affect
585 individuals of the different genotypes of *O. universa* to varying degrees, we could not detect any
586 systematic change in ρ_A in the data presented here.

587 The *O. universa* weight-area data of our study are compared with those of Marshall et al. (2015) from
588 Cariaco Basin sediment trap specimens, including *O. universa* Type I (M_{thick}) and Type III (M_{thin})
589 specimens, suggesting thinner test walls in the latter. In the area range of $3 \cdot 10^5 – 4 \cdot 10^5$ µm^2, our weight
590 data coincide with the expected Mediterranean Type III variety (Fig. S4c; Marshall et al., 2015), but at
591 $2 \cdot 10^5 – 2.5 \cdot 10^5$ µm^2 we see a mix of both types until at $1.5 \cdot 10^5$ µm^2 Type I coincides more with our results
592 (Fig. S4c; Marshall et al., 2015). We suggest that different groups of the Mediterranean *O. universa*
593 variety coexist in the Mediterranean with differences in the wall thickness.

594 The various interfering effects, which control the ρ_A of *O. universa* in the Mediterranean Sea, may also
595 explain differences in the weight-long axis relation data reported from other regions of the world ocean:
596 Bijma et al. (2002) weighed *O. universa* in the 500–600 µm size fraction in the Caribbean Sea and
597 reported a weight ranging from 28 to 60 µg. Lombard et al. (2010) measured a weight of 20–70 µg for
598 specimens sampled off Catalina Island, California, in the same size fraction of 500–600 µm. Our weight-
599 long axis relation data range from 24 to 45 µg (Fig. S3c) for the same size fraction of 500–600 µm,
600 ranging at the lower limit of the weight-long axis relations measured in the Caribbean (Bijma et al., 2002)

601 and off California (Lombard et al., 2010), which may be caused either by differences in genotypes or
602 environmental conditions, or both. Thinner walls overall in our specimens with respect to the mentioned
603 studies could be a possible explanation for the differences in ρ_A (Marshall et al., 2015). In our samples
604 from the Mediterranean, individuals exceeding 60 µg have long axis larger than 650 µm. The reason why
605 the ρ_A of *O. universa* is particularly low and highly variable in the Mediterranean despite high carbonate
606 ion concentration ($[CO_3^{2-}]$) and pH (Fig. 1) might be sought in factors other than, and in addition to,
607 chemical and physical conditions, namely the changing availability of food along the transect from the
608 Atlantic Ocean to the Levantine Basin.

609 5.3.2 Factors affecting the ρ_A of *G. ruber* (white) and *G. bulloides*

610 In the same way as in *O. universa*, the ρ_A of *G. ruber* (white)is only partly controlled by carbonate
611 chemistry, being instead affected by other factors like food availability. However, in contrast to *O.*
612 *universa*, the ρ_A data of *G. ruber* and *G. bulloides* follow systematic correlations. High ρ_A in the Atlantic
613 and Tyrrhenian Sea correlates with enhanced primary production (enhanced fluorescence, Fig. 1d; Fig.
614 7g) and presumably enhanced food availability (Fig. 6; Fig. 7g; Fig. 2, also noticeable in Fig. S2d-e and
615 Fig. S4d-e). At the same sites, larger IQR indicates more variability in test calcite production of *G. ruber*
616 (white) specimens, although a limited number of samples together with the low and uneven sampling size
617 impede any further interpretation of the data (Fig. 6). Under more oligotrophic conditions, low ρ_A of *G.*
618 *ruber* (white) might be caused by limited food availability. An opposite trend occurs in *G. ruber* (white)
619 sediment trap samples from the Madeira Basin, in which, apart from showing a negative significant
620 correlation between calcification intensity and productivity, ρ_A shows a positive correlation with
621 temperature (Weinkauf et al., 2016).

622 The relationship between food availability and ρ_A in *G. bulloides* is opposite to that in *G. ruber* (white)
623 (Fig. 6; Fig. 7g-h). The ρ_A of *G. bulloides* tests increases from the Atlantic toward the eastern
624 Mediterranean. At the same time, variability in ρ_A data increases with increasing absolute ρ_A, which
625 resembles the distribution of data in *G. ruber* (white) (Fig. 6): In both species larger IQRs are found
626 toward higher absolute ρ_A.

627 An opposite trend in ρ_A of the two species *G. ruber* (white) and *G. bulloides* had earlier been described
628 from the Arabian Sea, and could neither be assigned to changes in $[CO_3^{2-}]$ of ambient seawater nor
629 growth conditions (Beer et al., 2010a). Due to its symbionts, *G. ruber* would rather have an advantage
630 over symbiont-barren *G. bulloides* in oligotrophic waters, and support formation of test calcite through
631 CO_2 consumption and increasing $[CO_3^{2-}]$ and pH (see also Köhler-Rink and Kühl, 2005). Those findings
632 may still point toward differences in growth conditions: Reproduction of both *G. ruber* and *G. bulloides*
633 might be retarded under less optimal conditions, and additional calcite layers might be added to the
634 proximal test surface before reproduction, similar to the process described for *O. universa* (see above).
635 Therefore, tests may grow heavier under less than optimal food availability, given that carbonate
636 chemistry of ambient seawater does not seems to limit the formation of test calcite in our samples.

637 Comparing weight-long axis relations, *G. ruber* (255–350 µm size fraction) from plankton tows of the
638 western Arabian Sea have an average weight of 11.5 ±0.69 µg (de Moel et al., 2009), which is heavier
639 than the individuals from our study (5.9 ±0.31 µg; Fig. S3a; Appendix A). The difference in weight-long
640 axis relation may indicate that *G. ruber* was produced under more suited conditions for shell calcite
641 formation in the Arabian Sea especially during non-upwelling periods and still higher overall primary
642 productivity and food availability. However, the comparison might be biased by the fact that *G. ruber*
643 (white) and *G. elongatus* were analyzed together in the study of de Moel et al. (2009).

644 Data for supra-regional comparison of weight-long axis relation of *G. bulloides* from the water column
645 are found for the 200–250 µm size fraction: in the north Atlantic (56-63 °N) in June 2009 (Aldridge et al.,
646 2012) with a range of 1.75–2.92 µg (r^2 = 0.52). For that size fraction our results (36 °N) show heavier
647 tests in the Alboran Sea (3.46 ±0.15 µg), and similar weights at the Strait of Gibraltar (2.57 ±0.00 µg; Fig.
648 S3b). For the same water depth as in our samples, Schiebel et al. (2007) found heavier average weight-
649 long axis relation in fall (5.19 ±0.25 µg) than during spring (4.21 ±0.2 µg) in the eastern north Atlantic
650 (47 °N), and 5.51 ±0.31 µg during the SW monsoon in the Arabian Sea (16 °N). In general, higher ρ_A
651 occurs at lower latitudes and lower ρ_A at higher latitudes (see also Schmidt et al., 2004). All of these
652 findings support our idea of an effect of limited alimentation on calcification. Increased longevity and
653 ongoing production of additional calcite layers at the proximal side of shells may result in an increased
654 ρ_A, given that seawater carbonate chemistry only partially affecting the calcite formation in planktic
655 foraminifera in our samples.

656

657

658 ## 6. Conclusions

659 Absolute and relative abundances of planktic foraminifera were studied from plankton tow samples across
660 the Mediterranean in May 2013. The samples show large differences in species abundance and
661 assemblages between the different basins and sub-basins of the Mediterranean Sea. Absolute abundance
662 and diversity of planktic foraminifer assemblages are low in comparison to other regions of the world
663 ocean. Average standing stocks in the upper 200 m of the water column range from 1.42 ±1.43 ind.·10 m^{-3},
664 including twelve morphospecies in total. Planktic foraminifer assemblages are indicative of changing
665 temperatures and salinities, as well as trophic conditions, between the eastern and the western
666 Mediterranean Sea. Highest standing stocks of total planktic foraminifera occurred in the Strait of
667 Gibraltar and the Alboran Sea. Overall, the largest foraminifera tests occurred in the western part of the
668 transect, driven by the assemblage composition, and the presence of large *G. inflata*.

669 *Globigerinoides ruber* was the most abundant species; its dominance in the east compared to the west, is
670 likely caused by stratification of the surface water column, enhanced SST, and trophic conditions. *G.*
671 *ruber* is a symbiont-bearing species, which might be an advantage over symbiont-barren species like *G.*
672 *bulloides* under oligotrophic and food-limited conditions as in the Levantine Basin. *G. bulloides* was
673 more abundant in upwelled waters in the Strait of Gibraltar, in the Alboran Sea, and in the western

674 Mediterranean. *O. universa* was present at rather balanced standing stocks along the entire transect from
675 the west to the east. In general, distribution patterns of the main planktic foraminiferal species in the
676 Mediterranean seem to be mainly related to a combination of food availability and temperature.

677 In the Mediterranean supersaturated waters with respect to calcite and aragonite (Schneider et al., 2007;
678 Gemayer et al., 2015), foraminiferal calcification and ρ_A of the most frequent species, *G. ruber* (white)
679 and *G. bulloides*, are largely affected by trophic conditions and food availability. *G. ruber* is more affine
680 to oligotrophic conditions, and grows heaviest tests in less food-limited waters in the western basin near
681 Gibraltar and in the Tyrrhenian Sea. In contrast, *G. bulloides* grows heaviest tests under more food-
682 limited conditions in the eastern Mediterranean Sea. We speculate that reproduction is hindered when the
683 species-specific food sources are limited, while individuals continue adding calcite to the outer shell, and
684 grow heavier tests than individuals that reproduced earlier in ontogeny.

685 These observations highlight the need for more interdisciplinary studies on the causes of changing
686 foraminiferal assemblages and decreasing shell production, especially in the Mediterranean as a marginal
687 basin, which is assumed particularly sensitive to changes of the environment and global climate.

Appendices

Appendix A. Planktic foraminifera data from BONGO nets: relative and absolute abundances, and weight and size parameters. The nomenclature *G. bulloides* represents the *G. bulloides/G. falconensis* plexus, and *G. siphonifera* represents the *G. siphonifera/ G. calida/ G. radians plexus*.

Location	Atlantic	Gibraltar	Alboran Sea	South-Central Western Med.	Strait of Sardinia	Strait of Sicily	South of Ionian Sea	Off Southern Crete	Eastern Basin	Off Nile Delta	Off Lebanon	Antikythera Strait	Eastern Ionian Sea	Adriatic Sea	Otranto Strait	Northern Ionian Sea	Tyrrhenian Sea	North-Central Western Med.	Central Western Med.	Catalano-Balear
Station	1	2	3	5	6	7a	9	10	11	12	13	14	15	17	16	16-18	19	20	21	22
Absolute abundance (individuals*10 m^{-3})																				
Total numbers																				
G. ruber (white)	0.079	0.037	0.007	0.022	0	0	0.212	1.314	0.403	0.247	1.260	0.389	0.102	0	0.338	0	1.688	0	0	0
G. elongatus	0.118	0.019	0.007	0	0.024	0	0	0.282	0.054	0.027	0.202	0.269	0	0	0.182	0.070	0.537	0	0.025	0
T. sacculifer (without sac)	0.236	1.323	0.028	0	0.047	0	0.047	0.219	0.027	0.082	0.050	0	0	0.023	0.234	0	0.256	0	0.025	0
G. bulloides	0.148	2.311	0.456	0.501	0.142	0	0.165	0.094	0.054	0	0.076	0	0.102	0	0.052	0.023	0.307	0.197	0.102	0.147
G. inflata	0.118	0.503	3.514	0.545	0.449	0.358	0.071	0.125	0.027	0	0	0	0	0.023	0	0	0	0	0	0
O. universa	0.128	0.093	0.014	0.218	0	0.291	0	0.219	0.054	0.027	0.050	0	0.077	0.023	0.468	0.141	0.281	0.028	0.179	0.177
G. siphonifera	0.029	0.056	0.043	0.022	0	0.313	0	0.063	0	0	0.025	0	0	0	0	0	0	0	0.102	0
G. quadrilobatus	0.010	0.335	0.007	0.087	0	0.045	0.118	0.063	0.027	0	0	0	0	0.023	0	0	0.230	0.112	0.204	0.236
H. pelagica	0	0	0	0	0	0	0	0.125	0	0.027	0	0	0	0	0	0	0	0	0	0
T. sacculifer (with sac)	0	0	0	0	0	0	0	0	0	0	0	0	0	0	0	0	0.026	0	0	0
G. ruber (pink)	0	0.075	0	0	0.024	0	0.024	0.125	0	0.027	0	0.120	0	0	0	0	0	0	0	0
G. menardii	0	0	0	0	0	0	0	0	0	0	0	0	0	0	0	0	0	0	0	0.029
Unknowns	0.118	0.447	0.064	0.065	0.024	0	0.047	0.375	0.108	0	0.025	0.120	0.026	0.023	0.208	0.023	0.281	0.028	0	0.088
Total	0.985	5.120	4.141	1.460	0.709	1.006	0.683	3.003	0.753	0.439	1.689	0.898	0.307	0.114	1.482	0.258	3.607	0.365	0.638	0.678
150-350 µm size fraction																				
G. ruber (white)	0.030	0.037	0.007	0.022	0	0	0.212	1.314	0.403	0.247	1.109	0.389	0.102	0	0.338	0	1.560	0	0	0
G. elongatus	0.020	0	0	0	0.024	0	0	0.282	0.054	0.027	0.202	0.269	0	0	0.182	0.047	0.460	0	0.026	0
T. sacculifer (without sac)	0.148	1.174	0.029	0	0.047	0	0	0.188	0.027	0.082	0.050	0	0	0.023	0.234	0	0.230	0	0.026	0
G. bulloides	0.128	2.199	0.449	0.415	0.142	0	0.165	0.094	0.054	0	0.076	0	0.102	0	0.052	0.023	0.307	0.197	0.077	0.118
G. inflata	0.069	0.335	1.176	0.109	0.095	0.022	0	0.063	0	0	0	0	0	0.023	0	0	0	0	0	0
O. universa	0	0.075	0.007	0.087	0	0	0	0.094	0	0	0	0	0	0	0.208	0	0.026	0	0.026	0
G. siphonifera	0	0.019	0.029	0	0	0.022	0	0	0	0	0.025	0	0	0	0	0	0	0	0.102	0
G. quadrilobatus	0.010	0.280	0.007	0.087	0	0	0.071	0.063	0.027	0	0	0	0	0.023	0	0	0.230	0.112	0.204	0.236
H. pelagica	0	0	0	0	0	0	0	0.063	0	0	0	0	0	0	0	0	0	0	0	0
G. ruber (pink)	0	0.075	0	0	0.024	0	0.024	0.125	0	0.027	0	0.120	0	0	0	0	0	0	0	0
Total	0.404	4.193	1.703	0.719	0.331	0.045	0.471	2.284	0.564	0.384	1.462	0.778	0.205	0.068	1.014	0.070	2.814	0.309	0.459	0.354
350-500 µm size fraction																				
G. ruber (white)	0.049	0	0	0	0	0	0	0	0	0	0	0	0	0	0	0	0.051	0	0	0
G. elongatus	0.088	0.019	0.007	0	0	0	0	0	0	0	0	0	0	0	0	0.023	0.077	0	0	0
T. sacculifer (without sac)	0.079	0.130	0	0	0	0	0.047	0.031	0	0	0	0	0	0	0	0	0.026	0	0	0
G. bulloides	0.020	0.112	0.029	0.022	0	0	0	0	0	0	0	0	0	0	0	0	0	0	0.026	0.029
G. inflata	0.049	0.149	2.138	0.414	0.307	0.313	0.071	0.031	0.027	0	0	0	0	0	0	0	0	0	0	0
O. universa	0.049	0.019	0.007	0.109	0	0.067	0	0.125	0.027	0	0	0	0	0.023	0.130	0.023	0.153	0.028	0.051	0.118
G. siphonifera	0.020	0.019	0.007	0.022	0	0.201	0	0.031	0	0	0	0	0	0	0	0	0	0	0	0
G. quadrilobatus	0	0	0	0	0	0.022	0.047	0	0	0	0	0	0	0	0	0	0	0	0	0
H. pelagica	0	0	0	0	0	0	0	0.063	0	0.027	0	0	0	0	0	0	0	0	0	0
T. sacculifer (with sac)	0	0	0	0	0	0	0	0	0	0	0	0	0	0	0	0	0.026	0	0	0
G. menardii	0	0	0	0	0	0	0	0	0	0	0	0	0	0	0	0	0	0	0	0.029
Total	0.354	0.447	2.188	0.567	0.307	0.604	0.165	0.282	0.054	0.027	0	0	0	0.023	0.130	0.047	0.333	0.028	0.077	0.177

693 (**Appendix A**, cont.).

Location	Atlantic	Gibraltar	Alboran Sea	South-Central Western Med.	Strait of Sardinia	Strait of Sicily	South of Ionian Sea	Off Southern Crete	Eastern Basin	Off Nile Delta	Off Lebanon	Antikythera Strait	Eastern Ionian Sea	Adriatic Sea	Otranto Strait	Northern Ionian Sea	Tyrrhenian Sea	North-Central Western Med.	Central Western Med.	Catalano-Balear
Station	1	2	3	5	6	7a	9	10	11	12	13	14	15	17	16	16-18	19	20	21	22
>500 µm size fraction																				
G. ruber s.l.	0.010	0	0	0	0	0	0	0	0	0	0	0	0	0	0	0	0	0	0	0
T. sacculifer (without sac)	0.001	0.019	0	0	0	0	0	0	0	0	0	0	0	0	0	0	0	0	0	0
G. inflata	0	0.019	0.135	0.022	0.047	0.022	0	0.031	0	0	0	0	0	0	0	0	0	0	0	0
O. universa	0.079	0	0	0.022	0	0.224	0	0	0.027	0.028	0.050	0	0.077	0	0.130	0.117	0.102	0	0.102	0.059
G. siphonifera	0.010	0.019	0.007	0	0	0.089	0	0.031	0	0	0	0	0	0	0	0	0	0	0	0
G. quadrilobatus	0	0	0	0	0	0.022	0	0	0	0	0	0	0	0	0	0	0	0	0	0
Total	0.108	0.056	0.143	0.044	0.047	0.358	0	0.063	0.027	0.027	0.050	0	0.077	0	0.130	0.117	0.102	0	0.102	0.059
Relative abundance (%)																				
G. ruber (white)	8.00	0.72	0.17	1.49	0	0	31.03	43.75	53.57	56.25	74.63	43.33	33.33	0	22.81	0	46.81	0	0	0
G. elongatus	12.00	0.36	0.17	0	3.33	0	0	9.38	7.14	6.25	11.94	30.00	0	0	12.28	27.27	14.89	0	4.00	0
T. sacculifer (without sac)	24.00	25.45	0.69	0	6.67	0	6.90	7.29	3.57	18.75	2.99	0	0	20.00	15.79	0.00	7.09	0	4.00	0
G. bulloides	15.00	44.44	11.02	34.33	20.00	0	24.14	3.13	7.14	0	4.48	0	33.33	0	3.51	9.09	8.51	53.85	16.00	21.74
G. inflata	12.00	9.68	84.85	37.31	63.33	35.56	10.34	4.17	3.57	0	0	0	0	20.00	0	0	0	0	0	0
O. universa	13.00	1.79	0.34	14.93	0	28.89	0	7.29	7.14	6.25	2.99	0	25.00	20.00	31.58	54.55	7.80	7.69	28.00	26.09
G. siphonifera	3.00	1.08	1.03	1.49	0	31.11	0	2.08	0	0	1.49	0	0	0	0	0	0	0.00	16.00	0
G. quadrilobatus	1.00	6.45	0.17	5.97	0	4.44	17.24	2.08	3.57	0	0	0	0	20.00	0	0	6.38	30.77	32.00	34.78
H. pelagica	0	0	0	0	0	0	0	4.17	0	6.25	0	0	0	0	0	0	0	0	0	0
T. sacculifer (with sac)	0	0	0	0	0	0	0	0	0	0	0	0	0	0	0	0	0.71	0	0	0
G. ruber (pink)	0	1.43	0	0	3.33	0	3.45	4.17	0	6.25	0	13.33	0	0	0	0	0	0	0	0
G. menardii	0	0	0	0	0	0	0	0	0	0	0	0	0	0	0	0	0	0	0	4.35
Unknowns	12.00	8.60	1.55	4.48	3.33	0	6.90	12.50	14.29	0	1.49	13.33	8.33	20.00	14.04	9.09	7.80	7.69	0	13.04
Weight and size																				
G. ruber (white)																				
size fraction (µm)	250-300							200-250	200-250		200-250	250-300			250-300		200-250			
nº of individuals	1							4	4		4	2			4		4			
average size (µm)	285							221	215.25		221.5	281			268		218.5			
average weight (µg)	4.667							1.583	2.417		2	3.167			5.5		2.083			
SD (µg)	0.577							0.144	0.289		0	0.577			0		0.144			
size fraction (µm)	350-400							250-350	250-300		250-300	300-350					250-300			
nº of individuals	4							5	1		3	1					5			
average size (µm)	390							267	261		264	317					280.6			
average weight (µg)	14.333							3.867	2.667		5.111	6.667					4.8			
SD (µg)	0.289							0.115	0.577		0.192	0.577					0.2			
size fraction (µm)	400-450							300-350	350-400		300-350						300-350			
nº of individuals	1							3	1		2						5			
average size (µm)	412							313.333	356		323.5						343.4			
average weight (µg)	14.667							7.444	5.667		11						9.867			
SD (µg)	1.155							0.385	1.155		0						0.231			
size fraction (µm)								350-400									350-400			
nº of individuals								2									4			
average size (µm)								374									366			
average weight (µg)								8.833									9.083			
SD (µg)								0.764									0.144			

694

695 (**Appendix A**, cont.).

Location	Atlantic	Gibraltar	Alboran Sea	South-Central Western Med.	Strait of Sardinia	Strait of Sicily	South of Ionian Sea	Off Southern Crete	Eastern Basin	Off Nile Delta	Off Lebanon	Antikythera Strait	Eastern Ionian Sea	Adriatic Sea	Otranto Strait	Northern Ionian Sea	Tyrrhenian Sea	North-Central Western Med.	Central Western Med.	Catalano-Balear
Station	1	2	3	5	6	7a	9	10	11	12	13	14	15	17	16	16-18	19	20	21	22
size fraction (µm)																	400-450			
nº of individuals																	2			
average size (µm)																	413			
average weight (µg)																	16.167			
SD (µg)																	1.258			
G. bulloides																				
size fraction (µm)	300-350	200-250	200-250	350-400	300-350														400-450	300-350
nº of individuals	2	7	8	1	1														1	3
average size (µm)	326.5	228.143	227.875	364	337														414	318.333
average weight (µg)	4.5	2.571	3.458	4.667	4														11.667	8.222
SD (µg)	0.5	0	0.144	0.577	1														0.577	0.385
size fraction (µm)		250-300	250-300																	400-450
nº of individuals		12	2																	1
average size (µm)		263.75	270																	441
average weight (µg)		2.833	2.833																	20.333
SD (µg)		0	0.289																	1.155
size fraction (µm)		300-350	350-400																	
nº of individuals		2	4																	
average size (µm)		310.5	386.5																	
average weight (µg)		4.5	9.667																	
SD (µg)		0.5	0.144																	
size fraction (µm)		350-400	400-450																	
nº of individuals		2	2																	
average size (µm)		375.5	429																	
average weight (µg)		5.833	11																	
SD (µg)		0.289	0																	
size fraction (µm)		400-450	450-500																	
nº of individuals		1	1																	
average size (µm)		447	477																	
average weight (µg)		9.333	7.333																	
SD (µg)		0.577	0.577																	
O. universa																				
size fraction (µm)	350-400	250-300	500-550	400-450		450-500		300-350	350-400	700-750	650-700		700-750	450-500	300-350	400-450	400-450	400-450	450-500	350-400
nº of individuals	3	1	1	2		1		1	1	1	1		2	1	1	1	1	1	2	1
average size (µm)	390	286	501	445		479		342	398	719	687		722.5	452	347	444	441	441	479.5	377
average weight (µg)	17.667	7	20.667	11.667		31		3	6.333	47	43		24.167	14.333	5.333	18.667	24.333	22.667	31	20
SD (µg)	0.333	0	0.577	0.289		1		0	0.577	1	0		0.289	0.577	0.577	0.577	0.577	0.577	0.5	1
size fraction (µm)	400-450			450-500		500-550		350-400	500-550		750-800		750-800		350-400	550-600	450-500		550-600	400-450
nº of individuals	1			3		2		3	1		1		1		1	1	1		1	2
average size (µm)	444			479		539.5		373.667	539		781		785		369	559	455		571	425.5
average weight (µg)	28.667			22.889		33.833		6.556	25.667		54.667		53.667		6.667	34.333	23.667		45	24.167
SD (µg)	1.155			0.192		0.289		0.385	0.577		0.577		0.577		0.577	0.577	0.577		1	0.577
size fraction (µm)	500-550			650-700		600-650		400-450							400-450	600-650	500-550		650-700	450-500
nº of individuals	1			1		1		1							1	2	6		2	1
average size (µm)	527			656		603		439							412	640	534.5		676	482
average weight (µg)	36.667			25.667		50.667		13.667							13	54.833	30.278		84.333	35
SD (µg)	0.577			1.155		0.577		1.155							0	0.289	0.096		0.289	1
size fraction (µm)	550-600					650-700		450-500							450-500	650-700			750-800	500-550
nº of individuals	6					6		1							1	2			1	1
average size (µm)	578.667					674.333		460							476	656.5			762	509
average weight (µg)	45.389					47.889		17.333							24	63.333			136	42
SD (µg)	0.096					0.096		1.155							1	0.289			0	0
size fraction (µm)	600-650					700-750									500-550					
nº of individuals	1					2									3					
average size (µm)	605					720									527.333					
average weight (µg)	48.667					34									21.778					
SD (µg)	0.577					0									0.192					

696

697 (**Appendix A**, cont.).

Location	Atlantic	Gibraltar	Alboran Sea	South-Central Western Med.	Strait of Sardinia	Strait of Sicily	South of Ionian Sea	Off Southern Crete	Eastern Basin	Off Nile Delta	Off Lebanon	Antikythera Strait	Eastern Ionian Sea	Adriatic Sea	Otranto Strait	Northern Ionian Sea	Tyrrhenian Sea	North-Central Western Med.	Central Western Med.	Catalano-Balear
Station	1	2	3	5	6	7a	9	10	11	12	13	14	15	17	16	16-18	19	20	21	22
size fraction (µm)	650-700					750-800									550-600					
nº of individuals	1					1									1					
average size (µm)	651					772									570					
average weight (µg)	50.667					48									17.333					
SD (µg)	0.577					1									1.528					
size fraction (µm)															600-650					
nº of individuals															1					
average size (µm)															625					
average weight (µg)															23					
SD (µg)															0					
size fraction (µm)															650-700					
nº of individuals															2					
average size (µm)															654.5					
average weight (µg)															31.167					
SD (µg)															0.289					

698

Acknowledgments

We thank the captain and crew of the Spanish research vessel R/V Ángeles Alvariño. B. d'Amario is thanked for her software guidance and overall advice as well. The work was funded by the EC FP7 'Mediterranean Sea Acidification in a changing climate' project (MedSeA; grant agreement 265103).

References

Aldridge, D., Beer, C. J., and Purdie, D. A.: Calcification in the planktonic foraminifera *Globigerina bulloides* linked to phosphate concentrations in surface waters of the North Atlantic Ocean, Biogeosciences, 9, 1725-1739, 2012.

André, A., Quillévéré, F., Morard, R., Ujiié, Y., Escarguel, G., de Vargas, C., de Garidel-Thoron, T., and Douady, C.J.: SSU rDNA divergence in planktonic Foraminifera: Molecular taxonomy and biogeographic implications, PLoS One, 9 (8), doi: 10.1371/journal.pone.0104641, 2014.

André, A., Weiner, A., Quillévéré, F., Aurahs, R., Morard, R., Douady, C. J., Garidel-Thoron, T., Escarguel, G., de Vargas, C., and Kučera, M.: The cryptic and the apparent reversed: lack of genetic differentiation within the morphologically diverse plexus of the planktonic foraminifer *Globigerinoides sacculifer*, Paleobiology, 39 (1), 21-39, 2013.

Arnold, A. J. and Parker, W. C.: Biogeography of planktonic foraminifera, in: Modern Foraminifera, edited by: Gupta, B., Kluwer Academic Publishers, Dordrecht, Netherlands, 103-122, 1999.

Aurahs, R., Treis, Y., Darling, K., Kucera, M.: A revised taxonomic and phylogenetic concept for the planktonic foraminifer species *Globigerinoides ruber* based on molecular and morphometric evidence, Mar. Micropaleontol., 79, 1-14, 2011.

Auras-Schudnagies, A.D., Kroon, G., Ganssen, Ch., Hemleben, and J. van Hinte, Distributional pattern of planktonic foraminifers and pteropods in surface waters and top core sediments of the Red Sea, and adjacent areas controlled by the monsoonal regime and other ecological factors, Deep Sea Res., 36 (10), 1515–1533, 1989.

Bárcena, M.A., Flores, J.A., Sierro, F.J., Pérez-Folgado, M., Fabres, J., Calafat, A., and Canals, M.: Planktonic response to main oceanographic changes in the Alboran Sea (Western Mediterranean) as documented in sediment traps and surface sediments, Mar. Micropaleontol., 53, 423-445, 2004.

Bé, A. W. H.: An ecological, zoogeographic and taxonomic review of recent planktonic foraminifera, Oceanic Micropalaeontology, edited by Ramsay, A. T. S., 1, (1), 1–100, Academic Press, London, New York, San Francisco, 1977.

Bé, A. W. H. and Tolderlund, D. S.: Distribution and ecology of living planktonic foraminifera in surface waters of the Atlantic and Indian Oceans, in: The micropaleontology of oceans, edited by: Funnel, B. M. and Riedel, W. R., Cambridge University Press, London, U.K., 105-149, 1971.

Bé, A.W.H., Harrison, S.M., and Lott, L.: *Orbulina universa* (d'Orbigny) in the Indian Ocean, Micropaleontology, 19 (2), 150–192, 1973.

Beer, J., Schiebel, R., and Wilson, P. A.: Testing planktic foraminiferal shell weight as a surface water [CO_3^{2-}] proxy using plankton net samples, Geol. Soc. Am., 38, 103-106, 2010a.

Bijma, J., Faber, W.W., Hemleben, Ch.: Temperature and salinity limits for growth and survival of some planktonic foraminifers in laboratory cultures, J. Foraminifer. Res., 20 (2), 95–116, doi: 10.2113/gsjfr.20.2.95, 1990.

736 Bijma, J., Hönisch, B., and Zeebe, R. E.: Impact of the ocean carbonate chemistry on living foraminiferal shell weight: comment on
737 "carbonate ion concentration in glacial-age deep waters of the Caribbean Sea" by W. S. Broecker and E. Clark, Geochem. Geophy.
738 Geosy., 3 (11), 1064, doi: 10.1029/2002GC000388, 2002.

739 Boltovskoy, E. and Lena, H.A.: On the decomposition of the protoplasm and the sinking velocity of the planktonic foraminifers, Int.
740 Rev. Hydroviol., 55, 797-804, 1970.

741 Boltovskoy, E., Boltovskoy, D., and Brandini, F.: Planktonic foraminifera from south-western Atlantic epipelagic waters:
742 abundance, distribution and year-to-year variations, J. Mar. Biol. Ass. U.K., 79, 203-213, 2000.

743 Caromel, A. G. M., Schmidt, D. N., Phillips, J. C., Rayfield, E. J.: Hydrodynamic constraints on the evolution and ecology of
744 planktic foraminifera, Mar. Micropaleontol., 106, 69-78, 2014.

745 Cifelli, R.: Planktonic foraminifera from the Mediterranean and adjacent Atlantic waters (Cruise 49 of the Atlantis II, 1969), J.
746 Foramin. Res., 4, 171-183, 1974.

747 de Castro Coppa, M. G., Zei, M. M., Placella, B., Sgarella, F., and Ruggiero, E. T.: Distribuzione stagionale e verticale dei
748 foraminiferi planctonici del Golfo di Napoli, Boll. Soc. Natur. Napoli, 89, 1-25, 1980.

749 Cossarini, G., Lazzari, P., and Solidoro, C.: Spatiotemporal variability of alkalinity in the Mediterranean Sea, Biogeosciences, 12,
750 1647-1658, 2015.

751 Cramp, A., Collins, M., and West, R.: Late Pleistocene-Holocene sedimentation in the NW Aegean Sea: A palaeoclimatic
752 palaeoceanographic reconstruction, Palaeogeogr. Palaeoclimatol. Palaeocecol., 68, 61-77, 1988.
753

754 d'Orbigny, A. D.: Tableau méthodique de la classe des céphalopodes, Ann. Sci. Nat., Paris, Ser. 1, 7, 96-314, 1826.

755 Darling, K.F. and Wade, C.M.: The genetic diversity of planktic Foraminifera and the global distribution of ribosomal RNA
756 genotypes, Mar. Micropaleontol., 67 (3), 216– 238, 2008.

757 de Moel, H., Ganssen, G. M., Peeters, F. J. C., Jung, S. J. A., Kroon, D., Brummer, G. J. A., and Zeebe, R. E.: Planktic foraminiferal
758 shell thinning in the Arabian Sea due to anthropogenic ocean acidification?, Biogeosciences, 6, 1917-1925, 2009.

759 de Vargas, C., Norris, R., Zaninetti, L., Gibb, S. W., and Pawlowski, J.: Molecular evidence of cryptic speciation in planktonic
760 foraminifers and their relation to oceanic provinces, Proc. Natl. Acad. Sci. USA, 96, 2864-2868, 1999.

761 Dickson, A., G., and Millero, F. J.: A comparison of the equilibrium constants for the dissociation of carbonic acid in seawater
762 media, Deep-Sea Res., 34 (10), 1733-1743, 1987.

763 Gemayel, E., Hassoun, A. E. R., Benallal, M. A., Goyet, C., Rivaro, P., Saab, M. A., Krasakopoulou, E., Touratier, F., and Ziveri,
764 P.: Climatological variations of total alkalinity and total inorganic carbon in the Mediterranean Sea surface waters, Earth. Sys.
765 Dynam. Discuss., 6, 1499-1533, 2015.

766 Goyet, C., Hassoun, A. E. R., Gemayel, E.: Carbonate system during the May 2013 MedSeA cruise.
767 doi:10.1594/PANGAEA.841933, in supplement to: Hassoun, A. E. R., Guglielmi, V., Gemayel, E., Goyet, C., Saab, M. A., Giani,
768 M., Ziveri, P., Ingrosso, G., and Touratier, M.: Is the Mediterranean Sea circulation in a steady state, J. Water Res. Ocean Sci., 4 (1),
769 6-17, 2015b.

770 Glaçon, G., Vergraud-Grazzini, C., and Sigal, J.: Premiers resultants d'une série d'observations saisonnières des foraminifères du
771 plankton méditerranéen, in: Procceedings of the 2nd Plankton Conference, Rome, 1970, 555-581, 1971.

772 Goldstein, S. T.: Foraminifera: A biological overview, in: Modern Foraminifera, edited by: Gupta, B., Kluwer Academic Publishers,
773 Dordrecht, Netherlands, 37-55, 1999.

Grasshoff, K., Ehrhardt, M., Kremling, K.: Methods of seawater analysis, third ed., Verlag Chemie, Weinheim, Deerfield Beach, Florida, Basel, 1983.

Vergraud-Grazzini, C., Glaçon, C., Pierre, C., Pujol, C., and Urrutiaguer, M. J.: Foraminifères planctoniques de Méditerranée en fin d'été. Relations avec les structures hydrologiques, Mem. Soc. Geol. Ital., 36, 175-188, 1986.

Hassoun, A. E. R., Gemayel, E., Krasakopoulou, E., Goyet, C., Saab, M. A., Ziveri, P., Touratier, F., Guglielmi, V., and Falco, C.: Modeling of the total alkalinity and the total inorganic carbon in the Mediterranean Sea, J. Water Res. Ocean Sci., 4 (1), 24-32, 2015a.

Hassoun, A. E. R., Guglielmi, V., Gemayel, E., Goyet, C., Saab, M. A., Giani, M., Ziveri, P., Ingrosso, G., and Touratier, M.: Is the Mediterranean Sea circulation in a steady state, J. Water Res. Ocean Sci., 4 (1), 6-17, 2015b.

Hembelen, Ch., Spindler, M., and Anderson, O.R.: Modern Planktonic Foraminifera, Springer-Verlag, New York, Berlin, Heidelberg, 363 pp., 1989.

Hernández-Almeida, I., Bárcena, M. A., Flores, J. A., Sierro, F. J., Sanchez-Vidal, A., and Calafat, A.: Microplankton response to environmental conditions in the Alboran Sea (Western Mediterranean): One year sediment trap record, Mar. Micropaleontol., 78, 14-24, 2011.

Köhler-Rink, S. and Kühl, M.: The chemical microenvironment of the symbiotic planktonic foraminifer *Orbulina universa*, Mar. Biol. Res., 1, 68-78, 2005.

Kuroyanagi, A. and Kawahata, H.: Vertical distribution of living planktonic foraminifera in the seas around Japan, Mar. Micropaleontol., 53, 173-196, 2004.

Lewis, E., Wallace, D., and Allison, L. J.: Program developed for CO2 system calculations, Tennessee: Carbon Dioxide Information Analysis Center, managed by Lockheed Martin Energy Research Corporation for the US Department of Energy, 1998.

Lombard, F., Rocha, R. E., Bijma, J., and Gattuso, J. P.: Effect of carbonate ion concentration and irradiance on calcification in planktonic foraminifera, Biogeosciences, 7, 247-255, 2010.

Marshall, B. J., Thunell, R. C., Henehan, M. J., Astor, Y., and Wejnert, K. E.: Planktonic foraminiferal area density as a proxy for carbonate ion concentration: A calibration study using the Cariaco Basin ocean time series, Paleoceanography, 28, 363-376, 2013.

Marshall, B. J., Thunell, R. C., Spero, H. J., Henehan, M. J., Lorenzoni, L., Astor, Y.: Morphometric and stable isotopic differentiation of *Orbulina universa* morphotypes from the Cariaco Basin, Venezuela, Mar. Micropaleontol., 120, 46-64, 2015.

Mehrbach, C.: Measurement of the apparent dissociation constants of carbonic acid in seawater at atmospheric pressure, M.S., Oregon State University, Oregon, United States, 1973.

Mohan, R., Shetye, S. S., Tiwari, M., and Anilkumar, N.: Secondary calcification of planktic foraminifera from the Indian sector of Southern Ocean, Acta Geol. Sin.-Engl., 89 (1), 27-37, 2015.

Mojtahid, M., Manceau, R., Schiebel, R., Hennekam, R., and de Lange, G.J.: Thirteen thousand years of southeastern Mediterranean climate variability inferred from an integrative planktic foraminiferal-based approach: Holocene climate in the SE Mediterranean, Paleoceanography, 30 (4), 402–422, doi: 10.1002/2014PA002705, 2015.

Morard, R., Quillévéré, F., Escarguel, G., Ujiie, Y., Garidel-Thoron, T., Norris, R. D., and de Vargas, C.: Morphological recognition of cryptic species in the planktonic foraminifer *Orbulina universa*, Mar. Micropaleontol., 71, 148-165, 2009.

Morard, R., Qullévéré, F., Escarguel, G., Garidel-Thoron, T., de Vargas, C., and Kučera, M.: Ecological modeling of the temperature dependence of cryptic species of planktonic foraminifera in the Southern Hemisphere, Palaeogeogr. Palaeoclimatol. Palaeoecol., 391, 13-33, 2013.

Mortyn, P. G. and Charles, C. D.: Planktonic foraminiferal depth habitat and $\delta^{18}O$ calibrations: plankton tow results from the Atlantic sector of the Southern Ocean, Paleoceanography, 18 (2), 1037, doi: 10.1029/2001PA000637, 2003.

Moy, A.D., Howard, W.R., Bray, S.G., and Trull, T.W.: Reduced calcification in modern Southern Ocean planktonic Foraminifera, Nat. Geosci. 2, 276–280. doi: 10.1038/ngeo460, 2009.

NASA Goddard Space Flight Center, Ocean Ecology Laboratory, Ocean Biology Processing Group; (2013): MODIS-Aqua L2 Data; NASA Goddard Space Flight Center, Ocean Ecology Laboratory, Ocean Biology Processing Group. http://oceandata.sci.gsfc.nasa.gov/. Accessed on 06/06/2013.

Ottens, J. J.: April and August Northeast Atlantic surface water masses reflected in planktic foraminifera, Neth. J. Sea Res., 28 (4), 261-283, 1992.

Pados, T. and Spielhagen, R. F.: Species distribution and depth habitat of recent planktic foraminifera in Fram Strait, Artic Ocean, Polar Res., 33, 22483, doi: 10.3402/polar.v33.22483, 2014.

Papp A., Schmid M. E.: Die fossilien Foraminiferen des tertiären Beckens von Wien, Revision der Monographic von Alcide d'Orbigny (1846). Wien: Abhandlungen der Geologischen Bundesanstalt, 1985.

Parker, F. L.: Distribution of planktonic foraminiferal in some Mediterranean sediments, Pap. Mar. Biol. Oceanogr., 3, 204-211, 1955.

Pettersson, H.: The Swedish Deep-Sea Expedition, 1947-48, Deep-Sea Res., 1, 17-24, 1953.

Posgay, J. A.: The MARMAP Bongo zooplankton samplers, J. Northw. Atl. Fish. Sci., 1, 91-99, 1980.

Pujol, C. and Vergraud-Grazzini, C.: Distribution patterns of live planktic foraminifers as related to regional hydrography and productive systems of the Mediterranean Sea, Mar. Micropaleontol., 25, 187-217, 1995.

Rao, K. K., Jayalakshmy, K. V., and Kutty, M. K.: Ecology and distribution of recent planktonic foraminifera in eastern part of Arabian Sea, Indian J. Mar. Sci., 20, 25-35, 1991.

Rigual-Hernández, A., Sierro, F. J., Bárcena, M. A., Flores, J. A., and Heussner, S.: Seasonal and interannual changes of planktic foraminiferal fluxes in the Gulf of Lions (NW Mediterranean) and their implications for paleoceanographic studies: Two 12-year sediment trap records, Deep-Sea Res I, 66, 26-40, 2012.

Rio, D., Sprovieri, R., Thunell, R., Vergnaud-Grazzini, C., and Glaçon, G.: Pliocene-Pleistocene paleoenvironmental history of the western Mediterranean: A synthesis of ODP site 653 results, Proc. Ocean Drill Prog. Sci. Results, 107, 695-704, 1990.

Rohling E. J., Marino, G., and Grant, K. M.: Mediterranean climate and oceanography, and the periodic development of anoxic events (sapropels), Earth Sci., 143, 62-97, 2015.

Rohling, E., Ramadan, A., Casford, J., Hayes, A., and Hoogakker, B.: The marine environment: present and past, in: The physical geography of the Mediterranean, edited by: Woodward, J., Oxford University Press, New York, United States, 33-67, 2009.

Rohling, E.J., Sprovieri, M., Cane, T., Casford, J.S.L., Cooke, S., Bouloubassi, I., Emeis, K.C., Schiebel, R., Rogerson, M., Hayes, A., Jorissen, F.J., and Kroon, D.: Reconstructing past planktic foraminiferal habitats using stable isotope data: A case history for Mediterranean sapropel S5. Mar. Micropaleontol. 50 (1-2) 89-123, doi: 10.1016/S0377-8398(03)00068-9, 2004.

Schiebel, R. and Hemleben, C.: Modern planktic foraminifera, Palaeont. Z., 79 (1), 135-148, 2005.

Schiebel, R., Barker, S., Lendt, R., Thomas, H., and Bollmann, J.: Planktic foraminiferal dissolution in the twilight zone, Deep-Sea Res. II, 54, 676-686, 2007.

Schiebel, R., Hiller, B., and Hemleben, C.: Impacts of storms on recent planktic foraminiferal test production and $CaCO_3$ flux in the North Atlantic at 47ºN, 20ºW (JGOFS), Mar. Micropaleontol., 26, 115-129, 1995.

Schiebel, R., Waniek, J., Zeltner, A., and Alves, M.: Impact of the Azores Front on the distribution of planktic foraminifers, shelled gastropods, and coccolithophorids, Deep-Sea Res., 49, 4035-4050, 2002.

Schlitzer, R.: Ocean Data View, http://odv.awi.de,2016.

Schneider, A., Wallace, D. W. R., and Körtzinger, A.: Alkalinity of the Mediterranean Sea, Geophys. Res. Lett., 34, L15608, doi: 10.1029/2006GL028842, 2007.

Schneider, C.A., Rasband, W.S., Eliceiri, K.W. "NIH Image to ImageJ: 25 years of image analysis", Nature Methods 9, 671-675, 2012.

Schmidt, D. N., Thierstein, H. R., Bollmann, J., and Schiebel, R.: Abiotic forcing of plankton evolution in the Cenozoic, Science, 303, 207-210, 2004.

Schmuker, B. and Schiebel, R.: Spatial and temporal distribution of planktic foraminifers in the eastern Caribbean, Mar. Micropaleontol., 46, 387–403, 2002.

Shackleton, N.: Depth of pelagic foraminifera and isotopic changes in Pleistocene oceans, Nature, 218, 79–80, doi: 10.1038/218079a0, 1968.

Sousa, S. H. M., Godoi, S. S., Amaral, P. G. C., Vicente, T. M., Martins, M. V. A., Sorano, M. R. G. S., Gaeta, S. A., Passos, R. F., and Mahiques, M. M.: Distribution of living planktonic foraminifera in relation to oceanic processes on the southeastern continental Brazilian margin (23ºS-25ºS and 40ºW-44ºW), Continental Shelf Res., 89, 76-87, 2014.

Spero, H.J., Eggins, S.M., Russell, A.D., Vetter, L., Kilburn, M.R., and Hönisch, B.: Timing and mechanism for intratest Mg/Ca variability in a living planktic foraminifer, Earth Planet Sci. Lett., 409, 32–42, doi: 10.1016/j.epsl.2014.10.030, 2015.

Spero, H.J.: Ultrastructural examination of chamber morphogenesis and biomineralization in the planktonic foraminifer *Orbulina universa*, Mar. Biol., 99 (1), 9–20, 1988.

Spezzaferri, S., Kucera, M., Pearson, P. N., Wade, B. S., Rappo, S., Poole, C. R., Morard, R., and Stalder, C.: Fossil and genetic evidence for the polyphyletic nature of the planktonic foraminifera "*Globigerinoides*", and description of the new genus *Trilobatus*, PLOS One 10 (5), doi: 10.1371/journal.pone.0128108, 2015.

Thunell, R. C.: Distribution of recent planktonic foraminifera in surface sediments of the Mediterranean Sea, Mar. Micropaleontol., 3, 147-173, 1978.

van Raden, U. J., Groeneveld, J., Raitzsch, M, and Kučera, M.: Mg/Ca in the planktonic foraminifera *Globorotalia inflata* and *Globigerinoides bulloides* from Western Mediterranean plankton tow and core top samples, Mar. Micropaleontol., 78, 101-112, 2011.

Wang, L.: Isotopic signals in two morphotypes of *Globigerinoides ruber* (white) from the South China Sea: implications for monsoon climate change during the last glacial cycle, Palaeogeogr. Palaeoclimatol. Palaeoecol., 161, 381-394, 2000.

Weiner A. K. M., Weinkauf, M. F. G., Kurasawa, A., Darling, K. F., and Kucera, M.: Genetic and morphometric evidence for parallel evolution of the *Globigerinella calida* morphotype, Mar. Micropaleontol., 114, 19-35, 2015.

Weinkauf, M. F. G., Moller, T., Koch, M. C., and Kučera, M.: Calcification intensity in planktonic Foraminifera reflects ambient conditions irrespective of environmental stress, Biogeosciences, 10, 6639-6655, 2013.

889 Weinkauf, M. F. G., Kunze, J. G., Waniek, J. J., and Kucera, M.: Seasonal variation in shell calcification of planktonic foraminifera
890 in the NE Atlantic reveals species-specific response to temperature, productivity, and optimum growth conditions, PLOS One, 11
891 (2), doi: 10.1371/journal.pone.0148363, 2016.

892 Yáñez, M. V., Martínez, M. C. G., and Ruiz, F. M.: Cambio climático en el Mediterráneo español, edited by: Instituto Español de
893 Oceanografía, Ministerio de Educación y Ciencia, Madrid, España, 2010.

894 Zeebe, R. E.: History of Seawater Carbonate Chemistry, Atmospheric CO_2 and Ocean Acidification, Annu. Rev. Earth Planet. Sci.,
895 40, 141-165, 2012.

896 Ziveri, P., Grelaud, M.: Physical oceanography during Ángeles Alvariño cruise MedSeA2013, Universitat Autònoma de Barcelona,
897 doi: 10.1594/PANGAEA.846067.

898

Tables

Table 1. Date, time, location, volume filtered and environmental parameters of the sampled stations. Sea surface temperature (SST) and sea surface salinity (SSS) measured at 5 m depth. The remaining parameters are averaged from 5 to 200 depth with their respective SDs in parenthesis.

Leg	Station Code	Station Name	Day (DD/MM/YYYY)	Time	Latitude	Longitude	Volume (m^3)	Temperature (ºC)	SST (ºC)	Salinity (PSU)	SSS (PSU)	Fluorescense (µg/l)	pH	$[CO_3^{-2}]$ (mmol/kg)
1	1	Atlantic	03/05/2013	0:03	36º03'	-6º65'	1016	16.08 (0.84)	17.88	36.27 (0.10)	35.95	0.36 (0.32)	8.06 (0.05)	178.89 (22.25)
	2	Gibraltar	03/05/2013	12:47	35º94'	-5º56'	537	14.22 (1.05)	17.11	37.51 (0.81)	36.35	0.11 (0.06)	8.06 (0.02)	179.90 (6.15)
	3	Alboran Sea	05/05/2013	20:55	36º12'	-4º19'	1403	15.06 (1.17)	16.87	37.13 (0.68)	36.37	0.45 (0.44)	8.09 (0.03)	191.50 (13.84)
	5	South-Central Western Mediterranean	08/05/2013	10:44	38º54'	5º56'	459	14.33 (1.19)	16.99	37.95 (0.23)	37.65	0.18 (0.22)	8.10 (0.02)	200.36 (10.06)
	6	Strait of Sardinia	09/05/2015	20:34	38º27'	8º69'	423	14.34 (1.16)	17.50	38.23 (0.19)	37.77	0.19 (0.26)	8.08 (0.03)	199.89 (15.38)
	7a	Strait of Sicily	11/05/2013	0:20	37º04'	13º18'	447	15.12 (0.86)	17.27	38.16 (0.52)	37.43	0.23 (0.23)	8.09 (0.01)	207.14 (3.38)
	9	South of Ionian Sea	12/05/2013	11:31	35º12'	18º29'	425	16.17 (1.01)	19.53	38.78 (0.10)	38.64	0.13 (0.14)	8.12 (0.02)	232.36 (3.30)
	10	Off Southern Crete	14/05/2013	14:40	33º81'	24º27'	320	16.51 (1.44)	19.58	39.00 (0.39)	36.60	0.12 (0.19)	8.11 (0.01)	232.38 (8.43)
	11	Eastern Basin	15/05/2013	13:01	33º50'	28º00'	372	17.21 (1.30)	20.59	38.80 (0.44)	36.19	0.10 (0.07)	8.12 (0.02)	243.57 (10.26)
	12	Off Nile Delta	17/05/2013	3:14	33º22'	32º00'	364	17.59 (1.46)	21.82	38.99 (0.25)	37.45	0.15 (0.12)	8.11 (0.02)	239.99 (9.93)
	13	Off Lebanon	17/05/2013	16:15	34º23'	33º23'	397	17.35 (1.33)	21.58	38.73 (1.48)	no data	0.16 (0.13)	8.11 (0.02)	238.28 (7.52)
2	14	Antikythera Strait	20/05/2013	6:06	36º70'	23º42'	334	16.66 (1.21)	20.00	39.07 (0.03)	39.15	0.12 (0.08)	8.13 (0.01)	241.84 (6.26)
	15	Eastern Ionian Sea	21/05/2013	21:25	36º40'	20º81'	391	16.52 (1.31)	20.27	39.05 (0.01)	39.10	0.15 (0.15)	no data	no data
	17	Adriatic Sea	23/05/2013	21:09	41º84'	17º25'	440	14.67 (1.30)	18.76	38.82 (0.05)	39.12	0.20 (0.21)	8.10 (0.02)	218.53 (14.65)
	16	Otranto Strait	24/05/2013	23:49	40º23'	18º84'	385	15.67 (1.15)	19.49	38.70 (1.34)	30.47	0.16 (0.15)	8.13 (0.01)	236.93 (12.88)
	16-18	Northern Ionian Sea	25/05/2013	9:30	39º07'	18º70'	426	no data	no data	no data	no data	no data	no data	no data
	19	Tyrrhenian Sea	27/05/2013	12:40	39º83'	12º52'	391	14.74 (1.47)	18.60	38.30 (0.20)	37.97	0.18 (0.24)	8.12 (0.02)	216.97 (11.27)
	20	North-Central Western Mediterranean	29/05/2013	20:00	41º32'	5º66'	356	13.88 (0.94)	15.52	38.29 (0.20)	33.75	0.36 (0.24)	8.14 (0.02)	219.89 (11.27)
	21	Central Western Mediterranean	30/05/2013	10:30	40º07'	5º95'	392	13.98 (0.95)	16.78	37.66 (1.74)	37.37	0.17 (0.21)	8.11 (0.01)	204.41 (7.70)
	22	Catalano-Balear	31/05/2013	13:55	40º95'	3º32'	339	14.08 (1.33)	16.81	38.43 (0.08)	38.34	0.25 (0.39)	8.13 (0.02)	218.43 (13.11)

Figures

Fig. 1. **(a)** Temperature (ºC), **(b)** salinity, **(c)** fluorescence ($\mu g \cdot l^{-1}$), **(d)** pH, and **(e)** [CO_3^{2-}] ($\mu mol \cdot kg^{-1}$) values of the water column of the transect. Values follow a color scale (under every graph), also values shown in the isometric lines. X axis: water depth. Y axis: longitude (degrees). Measurement locations indicated with white dots, with the coinciding stations numbered at top. The station number and the map section are shown on the map (f). For station code names see Table 1. Note reversed color scale at (d) and (e). Software used: Ocean Data View (Schlitzer, 2016).

Fig. 2. Sampled stations with BONGO nets (dots). The numbers in the picture represent the station codes: First transect: 1 to 13, second transect: 14 to 22. For station code names see Table 1. Color scale at right represents the values of surface chlorophyll concentration (in µg/l), retrieved from *MODIS Aqua (L2),* from the closest day as possible, specified in the upper part, of the first transect.

Fig. 3. Absolute abundance of planktic foraminifera from BONGO nets during leg 1 (stations 1 to 13) and leg 2 (stations 22 to 14). Category 'Others' is comprised of *G. siphonifera/G. calida/ G. radians* plexus, *G. quadrilobatus*, *H. pelagica*, *G. ruber* (pink), *G. menardii* and *T. sacculifer* (with sac).

Fig. 4. Percentage of each planktic foraminifera size fraction in each station from (a) leg 1 and (b) leg 2. Sample size is indicated by *n* below each station code.

Fig. 5. Relative abundance of planktic foraminifera (%). Category 'Others' is comprised of *G. siphonifera/G. calida/ G. radians*, *G. quadrilobatus* plexus, *H. pelagica*, *G. ruber* (pink), *G. menardii* and *T. sacculifer* (with sac). Less than 1% values are not shown. Number in parenthesis indicates the total individuals of each location.

Fig. 6. Area density of *G. ruber* (white) and *G. bulloides* in box-and-whisker plots representation for the different location groupings in the Mediterranean. Box extends from the lower (Q_1) to upper (Q_3) quartiles values of the data, with a line at the median (Q_2). Whiskers extend from the quartiles to values comprised within a 1.5 interquartile range (IQR = $Q_3 - Q_1$) distance: $Q_1 - 1.5 \cdot IQR$; $Q_3 + 1.5 \cdot IQR$.

Fig. 7. Sample scores on the two PCA factors with the loadings of the environmental parameters on each factor represented by the red axis. The black axis represents the overlay of the absolute abundance values (individuals·10 m^{-3}) of every station of **(a)** all the foraminifera sample, **(b)** *G. inflata*, **(c)** *T. sacculifer* (without sac), **(d)** *G. ruber* (white), **(e)** *G. bulloides*, and **(f)** *O. universa*. Overlay of the Area density (ρ_A) values ($\mu g \cdot \mu m^{-2}$) of **(g)** *G. ruber* (white), **(h)** *G. bulloides*, and **(i)** *O. universa*. In blue colour western Mediterranean stations (incl. Atlantic and Strait of Gibraltar), in red color the eastern Mediterranean stations.

Figure 1

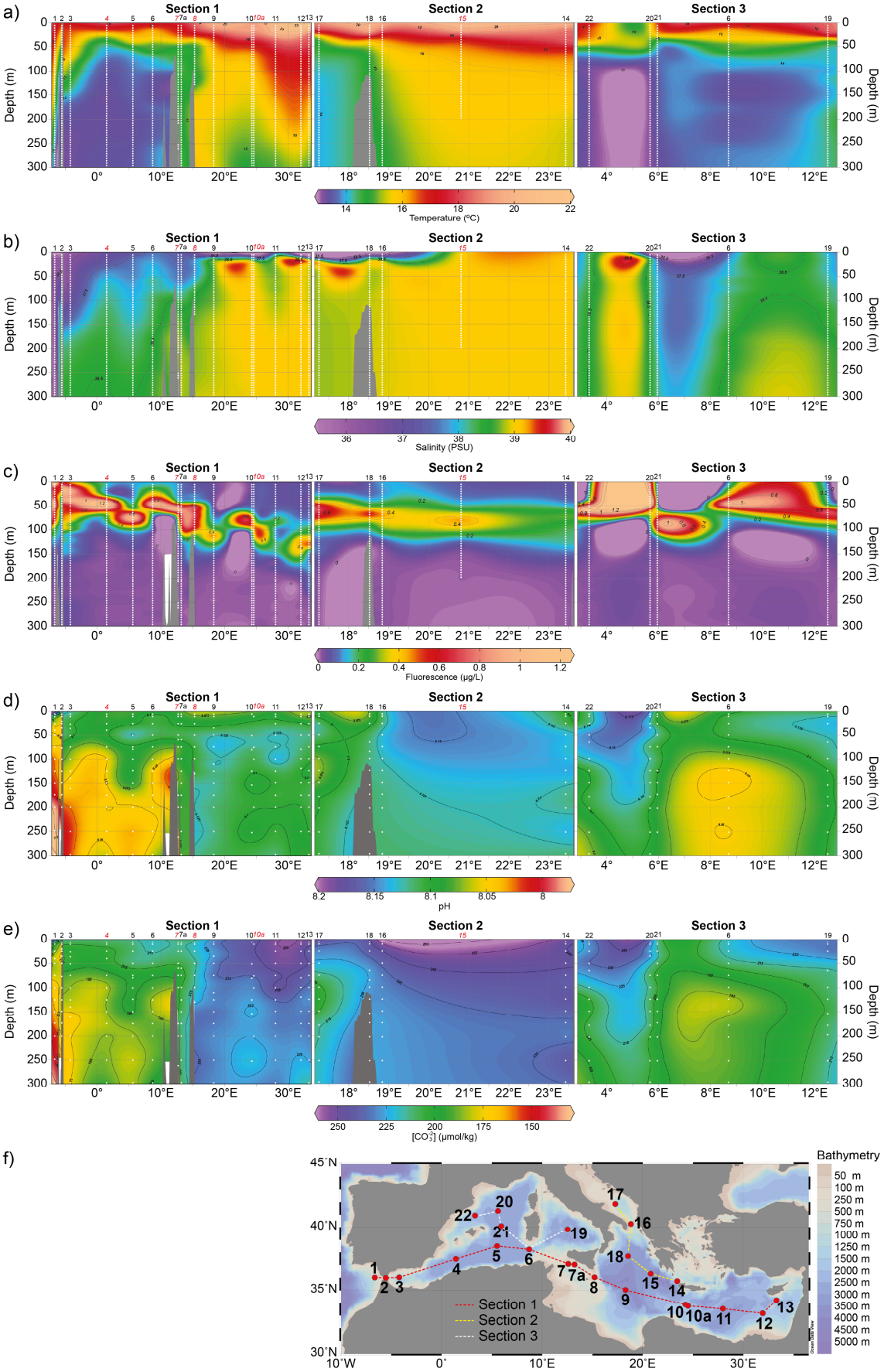
a)
Section 1
Section 2
Section 3
Depth (m)
Temperature (°C)
b)
Salinity (PSU)
c)
Fluorescence (µg/L)
d)
pH
e)
[CO3 2-] (µmol/kg)
f)
Bathymetry
50 m
100 m
250 m
500 m
750 m
1000 m
1250 m
1500 m
2000 m
2500 m
3000 m
3500 m
4000 m
4500 m
5000 m
Section 1
Section 2
Section 3

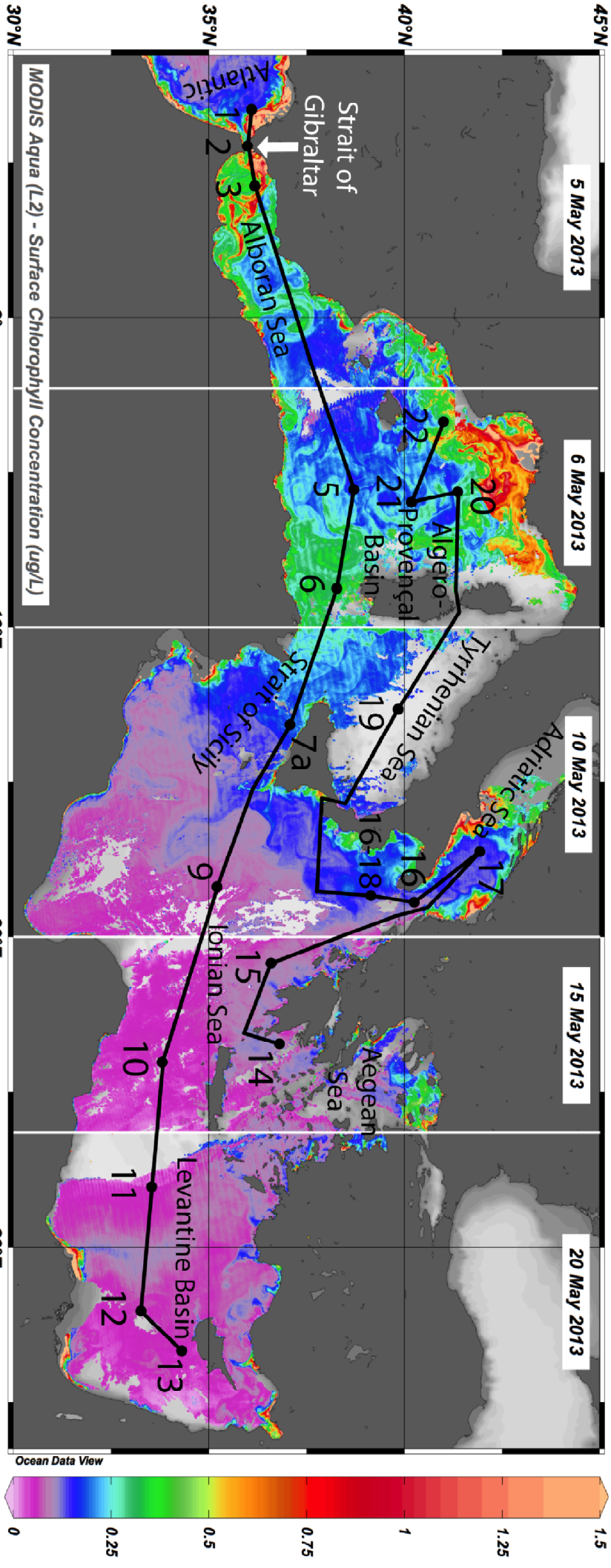
MODIS Aqua (L2) - Surface Chlorophyll Concentration (ug/L)
5 May 2013
6 May 2013
10 May 2013
15 May 2013
20 May 2013
Atlantic
Strait of Gibraltar
Alboran Sea
Algero-Provençal Basin
Tyrrhenian Sea
Strait of Sicily
Adriatic Sea
Ionian Sea
Aegean Sea
Levantine Basin
1
2
3
5
6
7a
9
10
11
12
13
14
15
16-18
16
17
19
20
21
22
30°N
35°N
40°N
45°N
0°
10°E
20°E
30°E
Ocean Data View
0
0.25
0.5
0.75
1
1.25
1.5

938 **Figure 2**

939 **Figure 3**

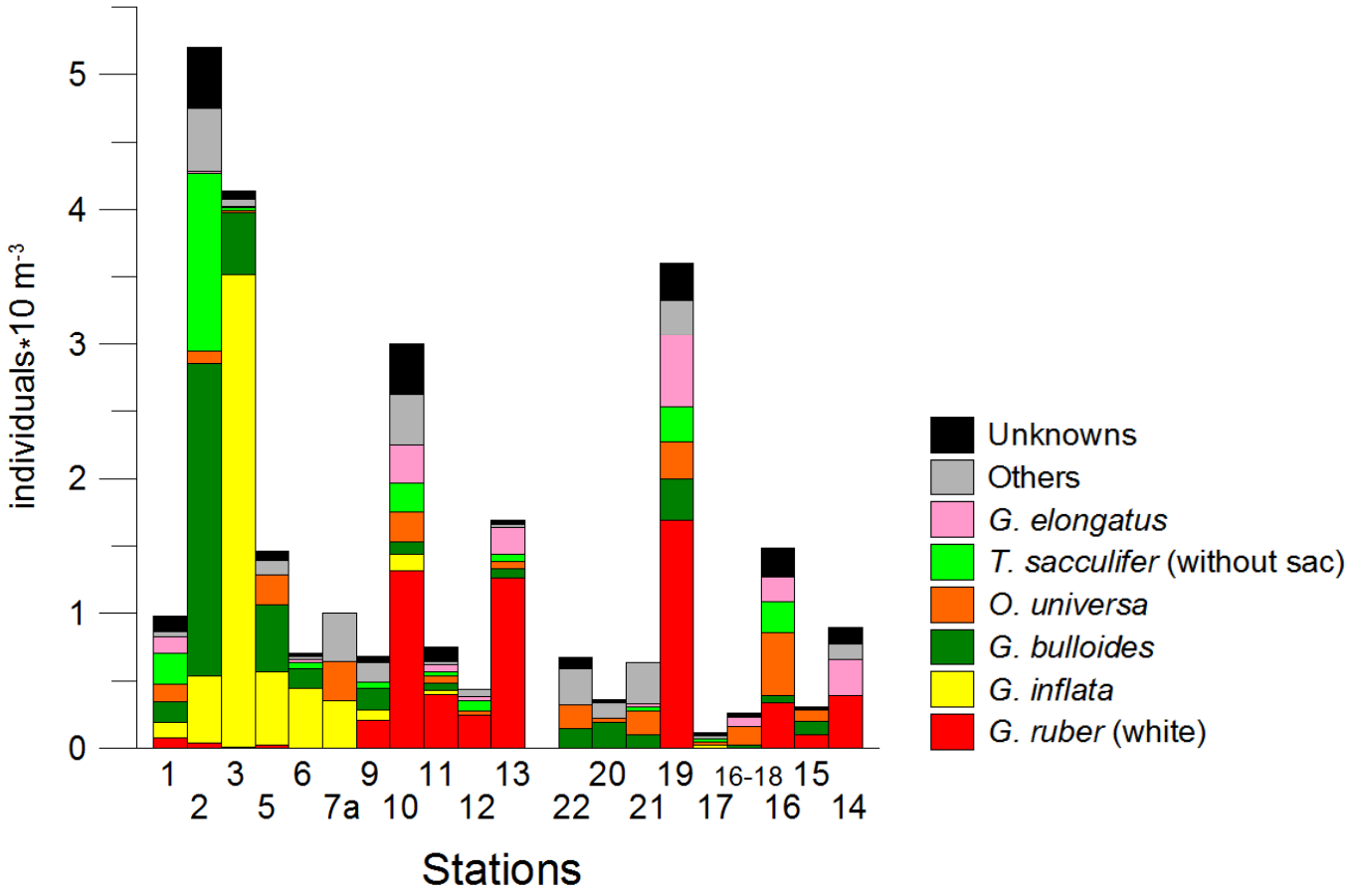
individuals*10 m-3
0
1
2
3
4
5
1
2
3
5
6
7a
9
10
11
12
13
22
20
21
19
17
16-18
16
15
14
Stations
Unknowns
Others
G. elongatus
T. sacculifer (without sac)
O. universa
G. bulloides
G. inflata
G. ruber (white)

940 **Figure 4**

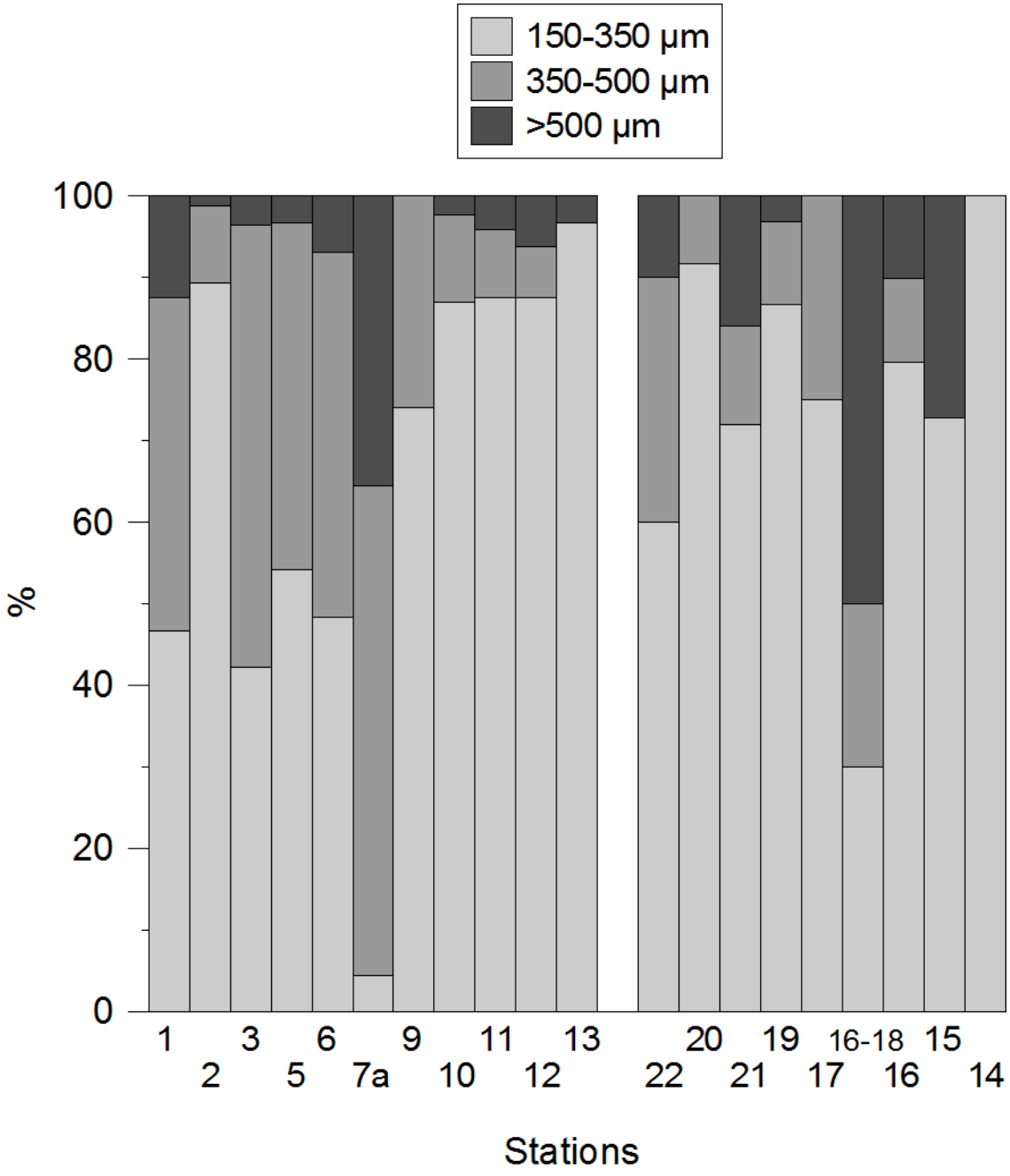
150-350 µm
350-500 µm
>500 µm
100
80
60
40
20
0
%
1
2
3
5
6
7a
9
10
11
12
13
20
22
19
21
16-18
17
15
16
14
Stations

941 **Figure 5**

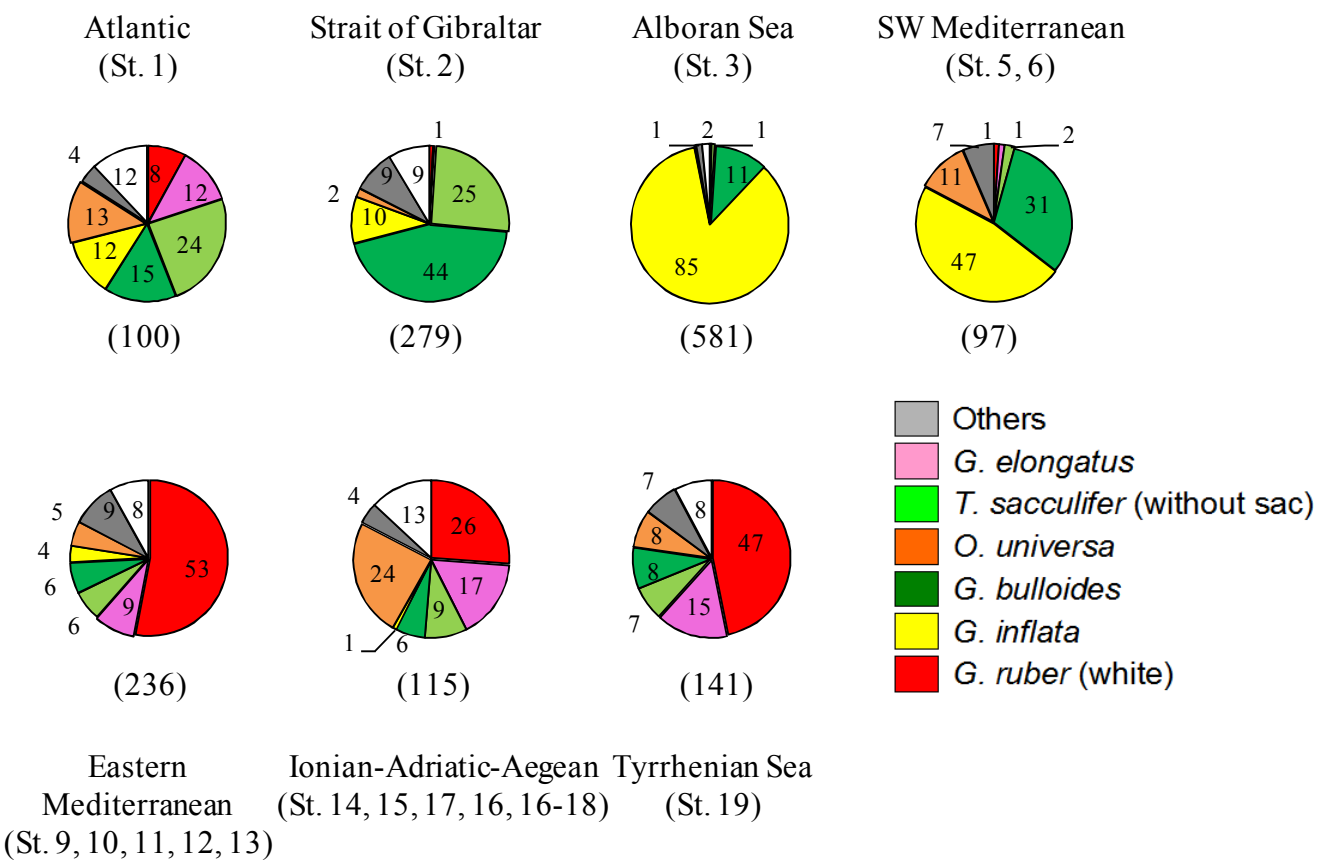
Atlantic
(St. 1)
Strait of Gibraltar
(St. 2)
Alboran Sea
(St. 3)
SW Mediterranean
(St. 5, 6)
(100)
(279)
(581)
(97)
(236)
(115)
(141)
Others
G. elongatus
T. sacculifer (without sac)
O. universa
G. bulloides
G. inflata
G. ruber (white)
Eastern Mediterranean
(St. 9, 10, 11, 12, 13)
Ionian-Adriatic-Aegean
(St. 14, 15, 17, 16, 16-18)
Tyrrhenian Sea
(St. 19)

942 **Figure 6**

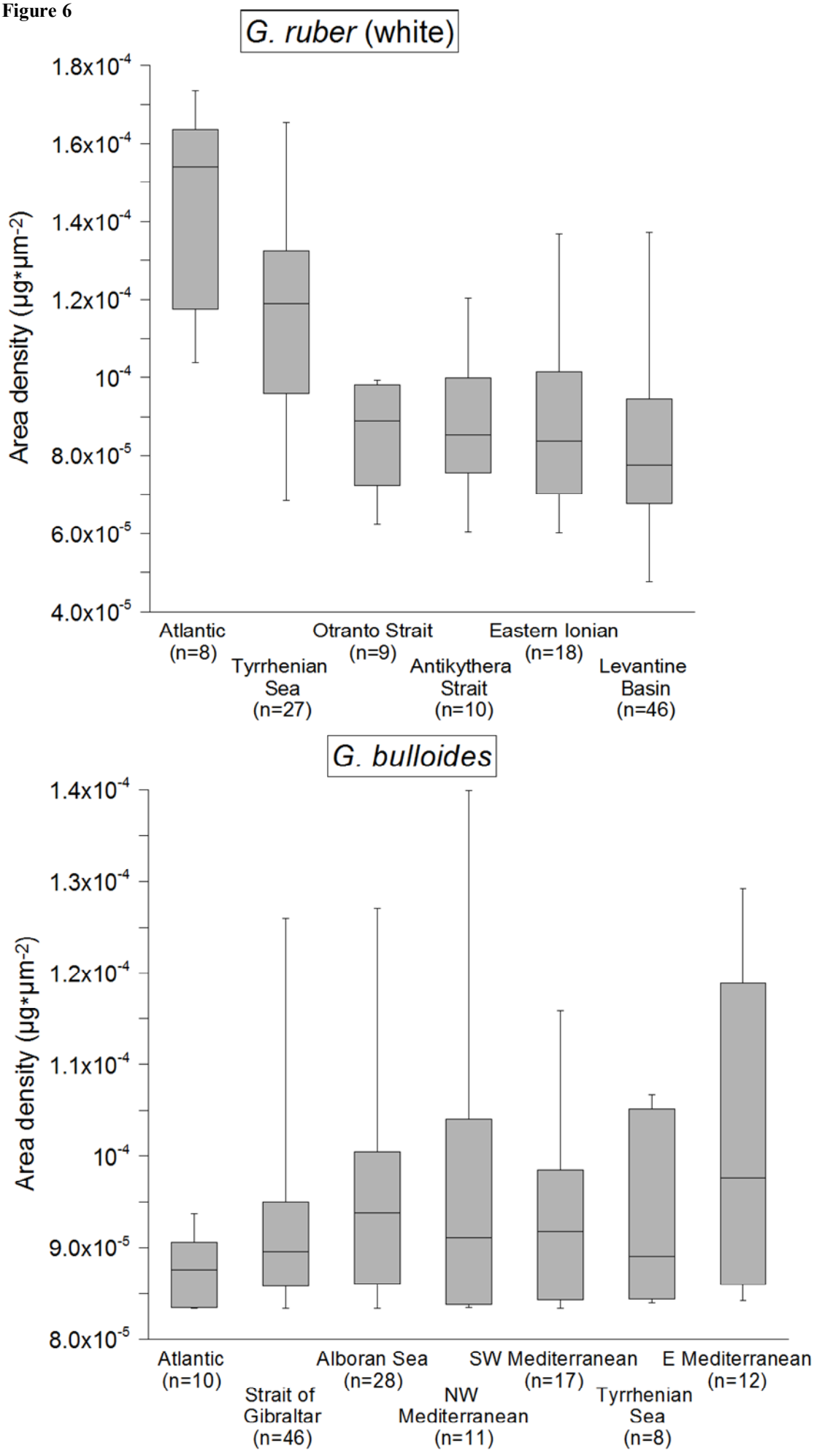
G. ruber (white)
Area density (µg*µm-2)
1.8x10-4
1.6x10-4
1.4x10-4
1.2x10-4
10-4
8.0x10-5
6.0x10-5
4.0x10-5
Atlantic (n=8)
Tyrrhenian Sea (n=27)
Otranto Strait (n=9)
Antikythera Strait (n=10)
Eastern Ionian (n=18)
Levantine Basin (n=46)
G. bulloides
Area density (µg*µm-2)
1.4x10-4
1.3x10-4
1.2x10-4
1.1x10-4
10-4
9.0x10-5
8.0x10-5
Atlantic (n=10)
Strait of Gibraltar (n=46)
Alboran Sea (n=28)
NW Mediterranean (n=11)
SW Mediterranean (n=17)
Tyrrhenian Sea (n=8)
E Mediterranean (n=12)

943 **Figure 7**

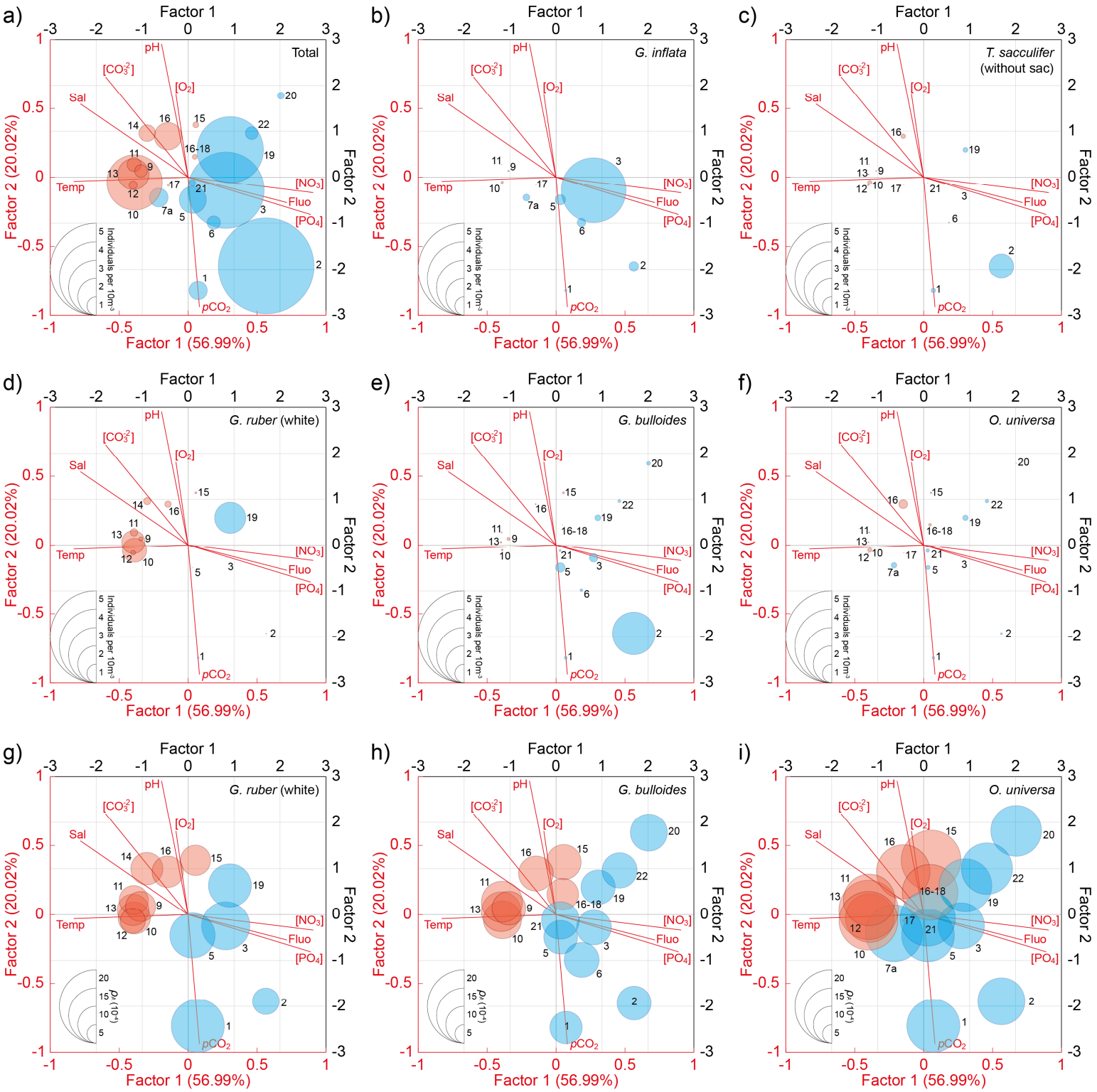
a)
Total
b)
G. inflata
c)
T. sacculifer (without sac)
d)
G. ruber (white)
e)
G. bulloides
f)
O. universa
g)
G. ruber (white)
h)
G. bulloides
i)
O. universa
Factor 1
Factor 2
Factor 1 (56.99%)
Factor 2 (20.02%)
pH
[CO3 2-]
[O2]
Sal
Temp
[NO3]
Fluo
[PO4]
pCO2
Individuals per 10m3
ρ (10+1)